NAVY DEPARTMENT
THE DAVID W. TAYLOR MODEL BASIN
WASHINGTON 7, D.C.

STUDY OF THE STRAIN AND MOTIONS OF THE USCGC CASCO AT SEA

by

Norman H. Jasper

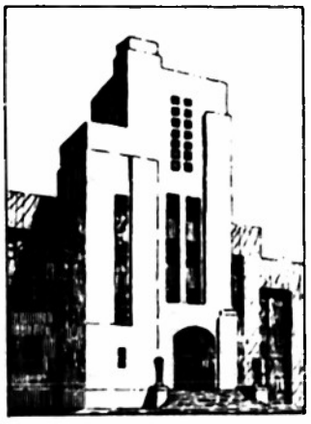

May 1953

Report 781

NS 731-037

STUDY OF THE STRAINS AND MOTIONS OF THE USCGC CASCO AT SEA

by

Norman H. Jasper

May 1953

Report 781
NS 731-037

TABLE OF CONTENTS

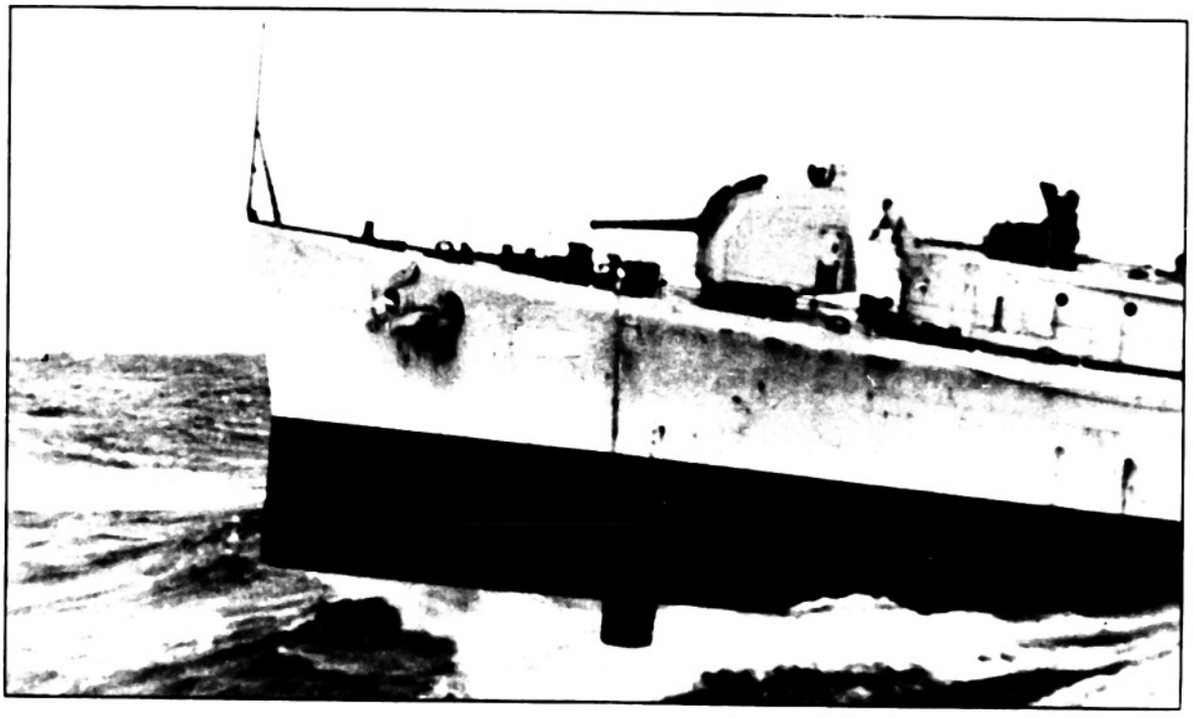

Slamming of USCG Cutter CASCO

ABSTRACT

This report presents and evaluates strain and motion data measured during the Spring of 1951 on the USCGC CASCO while on weather duty in the North Atlantic. The appended material evaluates the performance of recently developed automatic strain and motion measuring apparatus.

INTRODUCTION

The strength design of ships, which has passed through a gradual process of evolution, is still basically founded on empirical rules. The calculation of the longitudinal strength of a ship, if it is computed at all, is usually carried out by assuming that the ship is poised statically on some "standard" wave. This process is fairly satisfactory for comparing various ship designs but cannot be considered a realistic representation of the effect of actual sea conditions. There are numerous cases on record where ships have shown evidence of lack of longitudinal strength.

Information concerning the actual demands made upon a ship's hull girder when subjected to the action of the sea is neither sufficient nor in a form which can be used for a valid evaluation of the present method of ship design. Weaknesses in ships have often become apparent only after failures have occurred. It is necessary to determine the demands which the sea makes upon the hull girder and how these demands vary with the intended service of the vessel. When such information is available, the shipbuilder must be able to apply it to a more equitable design of the hull girder.

The problem confronting the ship designer is to design the ship girder to withstand the most severe loading that it is likely to encounter throughout its intended service and to do so in a manner which results in an equitable distribution of strength throughout the vessel. This design procedure not only should be based on probable service requirements but should also be economical.

Realizing the lack of reliable information on the actual strains and motions of ships at sea, the Bureau of Ships established a research project at the David Taylor Model Basin.[1] This project was for the purpose of making additional measurements of strains and motions of ships at sea and the development of improved methods of design of the ship girder and of its structural components in the light of the additional knowledge obtained.

It is apparent that this over-all study can become quite extensive. It was necessary for the Taylor Model Basin to study the over-all problem objectively and to decide upon a general program that could reasonably be accomplished with the available facilities, time, and funds. A preliminary outline of such a program was published in the August 1950 issue of the Journal of Naval Engineers.[2] As part of the project it was proposed to collect data on many

---

[1]References are listed on page 54.

ships operating on the various sea routes and under a variety of sea conditions. The data to be collected were to give an index to the ship's seaworthiness, to the acceleration experienced by the hull girder as a whole, and to the severity and distribution of stresses which the hull must withstand.

It would be impractical to secure this mass of data by direct oscillographic recording, as had been used in prior tests on ships at sea. It was therefore decided to develop instrumentation which would obtain the desired data automatically without requiring attending personnel. The objective was to provide an instrument that could be installed on a ship and then remain on it for the minimum time of a complete voyage, say one month, and from which the desired data could be removed at the end of that period. The required instrumentation, in addition to providing the proper information, should be sturdy, reliable, and economical in cost and operation.[2,3]

In accordance with this objective, the Taylor Model Basin has developed a number of devices:

1. The TMB Automatic Ship's Motion Recorder which records the output of several transducers as a function of time and does this for a predetermined duration at preselected intervals of time, that is, it performs a sampling operation.

2. The TMB Cycle Counter which may be used with a number of different types of transducers. The counter tabulates on digital counters the number of times that a given magnitude of cyclic variation has occurred. The original intention was to utilize the counter to analyze the strain variations in the hull girder according to the magnitudes of the strain variations. Another type of counter that was developed classifies the variations according to the magnitude of the cyclic variation as well as according to the mean value about which the variations occur.

3. A Mechanical Strain-Cycle Gage of 10-in. base length which is designed to work directly into the TMB cycle counter.

4. A Diaphragm Pressure Gage which is designed to measure pressures acting on the hull of the ship. The gage utilizes a differential transformer as the sensing element.

5. A Strain Gage of 10-in. base length which utilizes a differential transformer.

6. A Time-Totalizer which indicates directly the total time that the value of a time function, such as a strain, was greater than any one of a number of predetermined magnitudes.

At the request of the Bureau of Ships[4] the Coast Guard made a weather ship available for the purpose of evaluating the new instrumentation.[5]

The vessel selected for the test installation was the USCGC CASCO, formerly the U.S. Navy seaplane tender AVP 12. An inboard profile of the CASCO is shown in Figure 1. The ship has a length between perpendiculars of 300 ft, extreme beam of 41 ft 3/4 in. and design draft of 11 ft 7 1/16 in. The average displacement during the trials was 2460 tons, corresponding to a mean draft of 12 ft 2 1/2 in.

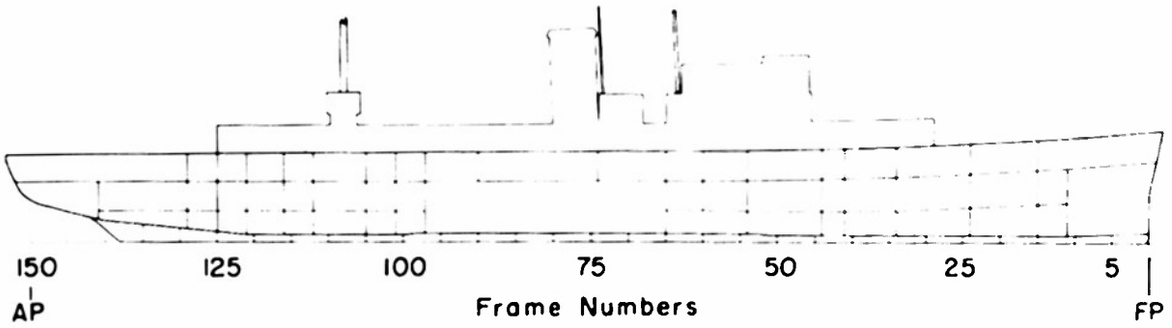

Figure 1 - Inboard Profile of USCGC CASCO
See Figure 3 for location of gage stations.

Ships of this class had evidenced some structural failures during their duty tours in the North Atlantic. Accordingly, in order to provide environmental conditions under which the automatic instrumentation could be evaluated, the test voyage was selected to encounter rough weather with realistically large strains and motions. The ship left Boston on 11 March 1951 and returned on 12 April 1951, having been, in the interim period, on weather and emergency rescue duty in the North Atlantic; the entire course is shown in Figure 2. Fairly heavy weather was encountered at the beginning of this period, but the sea was rather moderate toward the end of the trip. The quantities measured included strain near the forward quarterpoint and near amidships; heaving, rolling, and pitching accelerations; angles of roll and pitch; pressures acting on the bow; wind and sea conditions; and speed and heading of the ship.

It was the original intent of these particular tests to provide information for the evaluation of the performance and reliability of the pilot apparatus under service conditions. The data obtained, however, were to prove valuable in guiding the future development of this program and to help resolve a number of important questions. This report will concern itself primarily with an analysis of the strains and motions of the USCGC CASCO. To this end the data were studied with the following objectives in mind:

a. To determine the relative importance of hull-girder stresses associated with the rigid-body motions of the ship as against those associated with the flexural vibrations of the ship.

b. To determine whether the incidence of strain variations is such as to make endurance strength an important design consideration in hull girder design.

c. To determine typical patterns of time-strain variation in the hull girder.

d. To determine the pattern and incidence of bodily ship motions such as heave, pitch, and roll. In particular, it was desired to find a sampling period and sampling interval which would permit valid expansions of the sampled data.

e. To obtain some idea as to the regularity or lack of regularity of the sea.

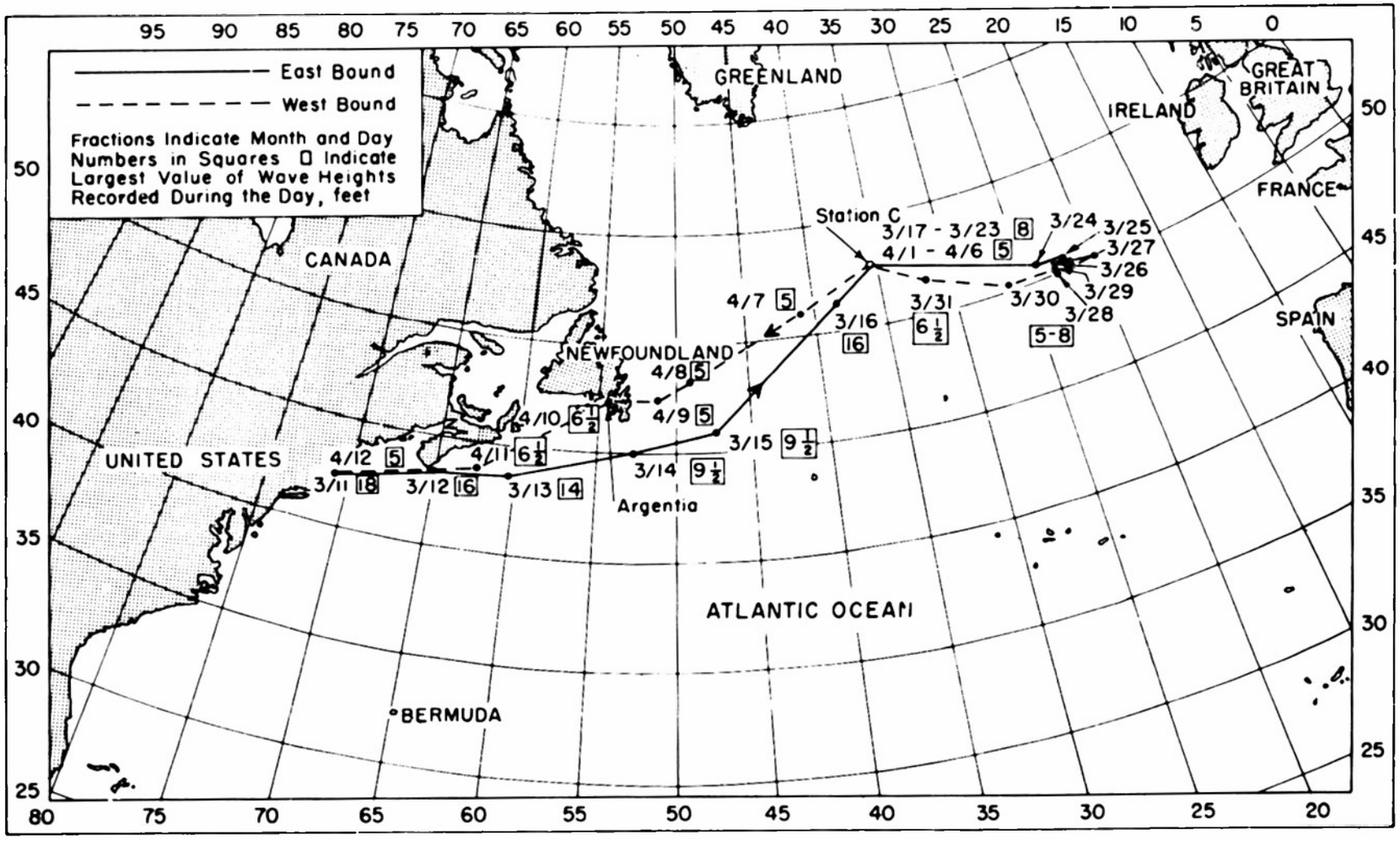

Figure 2 - Chart of the CASCO's Test Voyage

f. To compare the simultaneous strains in the hull near the forward quarterpoint and near amidships to determine their relative severity and the conditions under which severe straining of the hull does occur.

g. To compare measured strains with those computed by the standard strength calculation method.

h. To determine the pattern and magnitude of pressures acting on the bow, especially under conditions of slamming, and to observe the effect of slamming on hull stresses (strains)*

The several items of instrumentation used in these tests are described in Appendix 3 together with an evaluation of their performance.

INSTRUMENT INSTALLATION AND TEST PROCEDURE

In general, the shipboard instrument installation comprised two transverse belts of strain gages, one near Frame 41 and one near Frame 61. The former location is near the forward quarterpoint of the ship, and the latter was as close as practical to the midship section, Frame 75. In addition, a diaphragm pressure gage was installed in a plate next to the keel at Frame 23; prior local structural damage had indicated that this location was in a region of relatively large impact pressures. The ship's motion recorders and the roll and pitch pickups were installed in Compartment A207-1-L, Frames 60-65. Table 1 gives a list of the gage locations.

TABLE 1
Gage Locations

Station	Type of Gage	Location	
1	Strain Cycle Gage 107619	Main Deck Longitudinal, 8 ft stbd.	40 in. fwd of Frame 65
	Strain Cycle Gage 107621	Main Deck Longitudinal, 8 ft stbd.	58 in. fwd of Frame 65
	10-in. Variable Inductance Strain Gage	Main Deck Longitudinal, 8 ft stbd.	74 in. fwd of Frame 65
	SR-4 Wire Strain Gage	Main Deck Longitudinal, 8 ft stbd.	94 in. fwd of Frame 65
2	SR-4 Wire Strain Gage	Main Deck Longitudinal, 8 ft port	96 in. fwd of Frame 65
3	Strain Cycle Gage 107617	Top of Keel	32 in. fwd of Frame 65
	Strain Cycle Gage 107618	Top of Keel	48 in. fwd of Frame 65
	SR-4 Wire Strain Gage	Top of Keel	66 in. fwd of Frame 65
4	SR-4 Wire Strain Gage	Main Deck Longitudinal, 8 ft port	40 in. fwd of Frame 43
5	SR-4 Wire Strain Gage	Main Deck Longitudinal, 8 ft stbd.	40 in. fwd of Frame 43
6	SR-4 Wire Strain Gage	Top of Keel	40 in. fwd of Frame 43
7	Pressure Gage	In Shell Strake Adjacent to Keel	15 in. fwd of Frame 24 9 in. stbd of centerline
8	Schaevitz Accelerometer (to measure heave accelerations)	On centerline of ship	74 in. fwd of Frame 80 22 in. below 2nd Dec

*To avoid misunderstanding later on, it will be stated here that whenever the term "measured stress" is used in this report, a stress computed on the basis of measured strains is to be inferred. Whenever the term slamming is used, it denotes the phenomenon in which the ship's bottom, near the bow, first comes free of the sea and then, as the bow descends, is subjected to an impact by the oncoming sea.

Diagrams of the strain-gage installation are given in Figures 3 and 4 and photographs in Figures 5 and 6. It is seen that SR-4 strain gages, oriented to measure longitudinal strain,

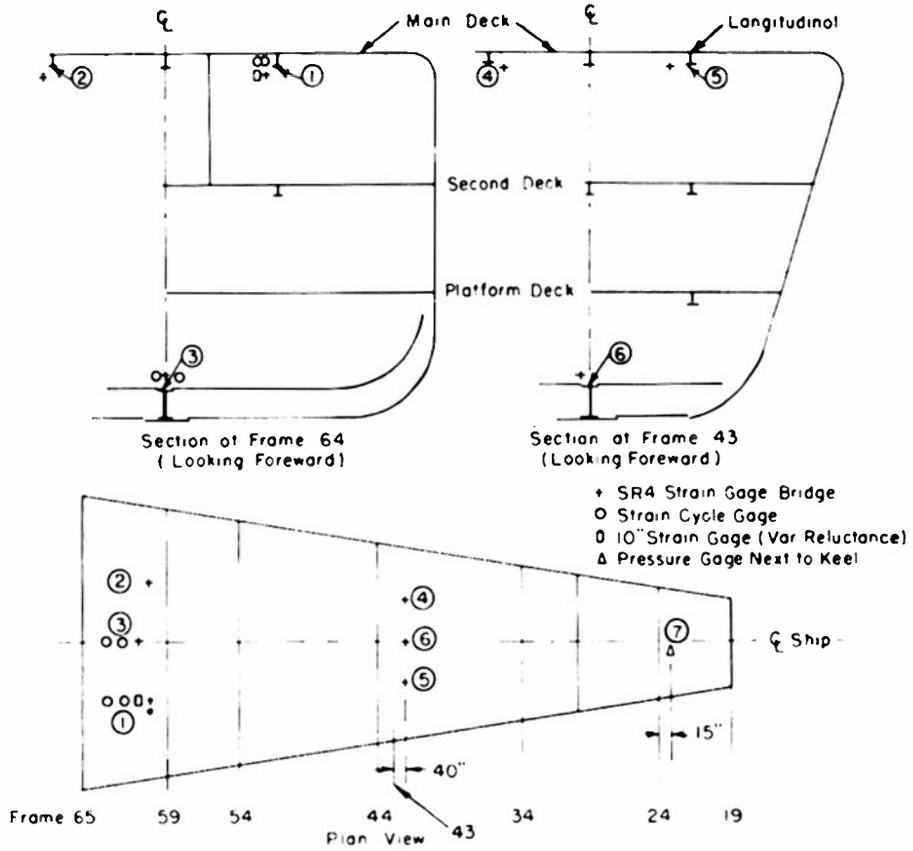

Figure 3 - Schematic Sketch of Gage Locations

The circled numbers represent station numbers (see Table 1).

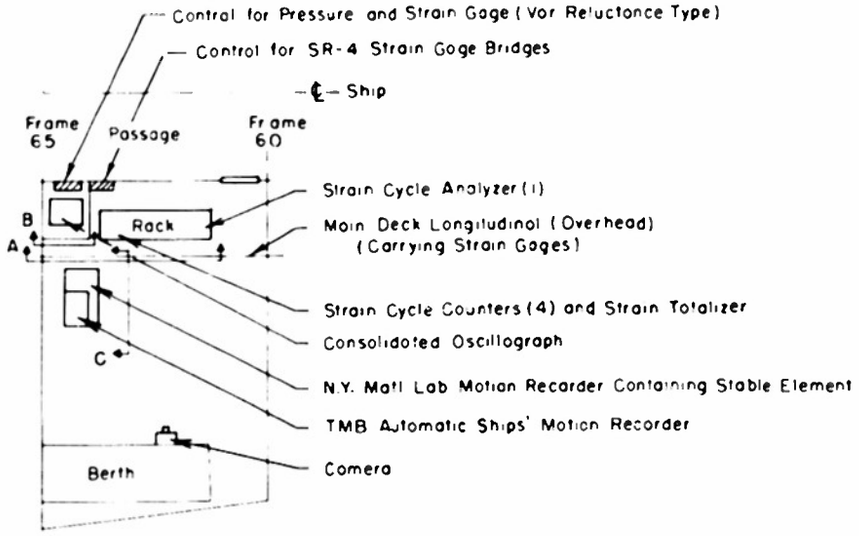

Figure 4 - Orientation of Equipment in the Central Station on Second Deck

Photographs taken at Sections A-A, B-B, and C-C are reproduced in Figures 7, 8, and 9, respectively.

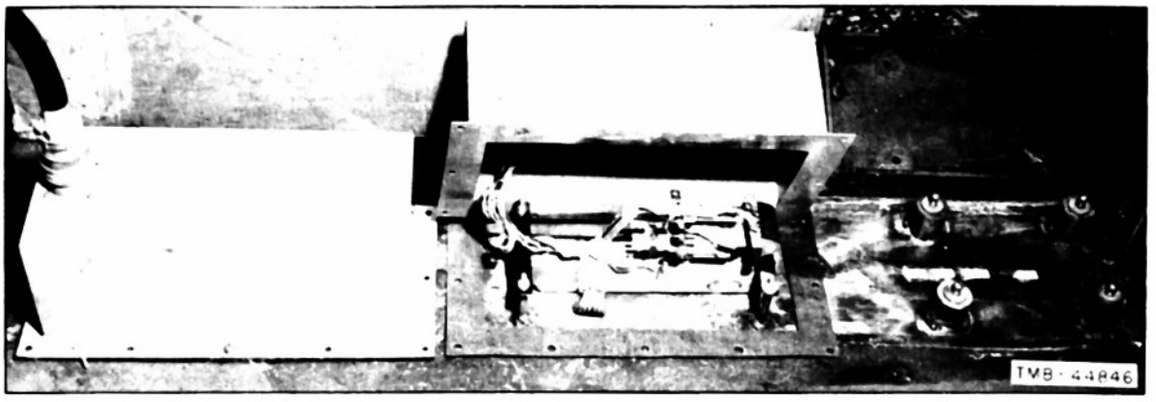

Figure 5 - Strain Gage Installation on Top of the Keel near Frame 65 (Station 3)

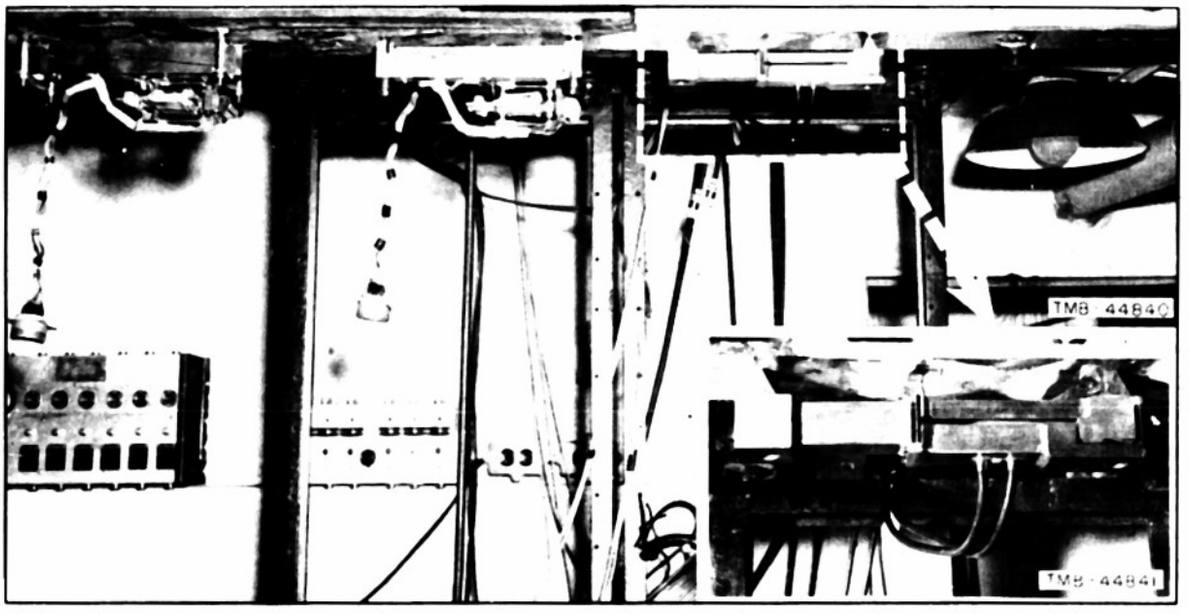

Figure 6 - Strain Gage Installation on Main Deck Longitudinal(s), near Frame 65 (Station 1)

were installed on the keel and on two main-deck longitudinals near Frames 41 and 61. Their output was recorded by a string oscillograph, thus permitting simultaneous measurement of all strain signals. The mechanical strain cycle gages were located next to the SR-4 strain gages, as shown in Figures 5 and 6, to permit some check between the two types of instrumentation. The strain-cycle gages were installed in pairs to provide a check on each other. The strain-cycle gages were also used to actuate the strain totalizer (see Figure 7). An experimental 10-in. strain gage, utilizing a differential transformer, was installed as shown on the right in the photograph (Figure 6). All the counting and recording equipment was located in Compartment A207-1-L, the central station. The general arrangement of the equipment at this station is shown in Figure 4; photographs of the various items of interest are given in Figures 6 to 9.

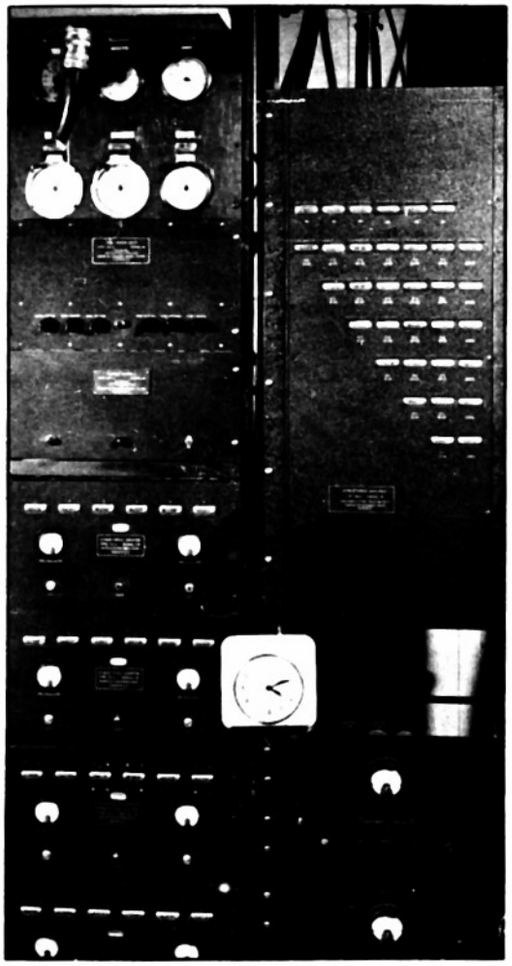

Figure 7 - Rack Mounting of Time (Strain) Totalizer, Strain-Cycle Counters, and Strain-Cycle Analyzer

See Figure 4 for location of this equipment.

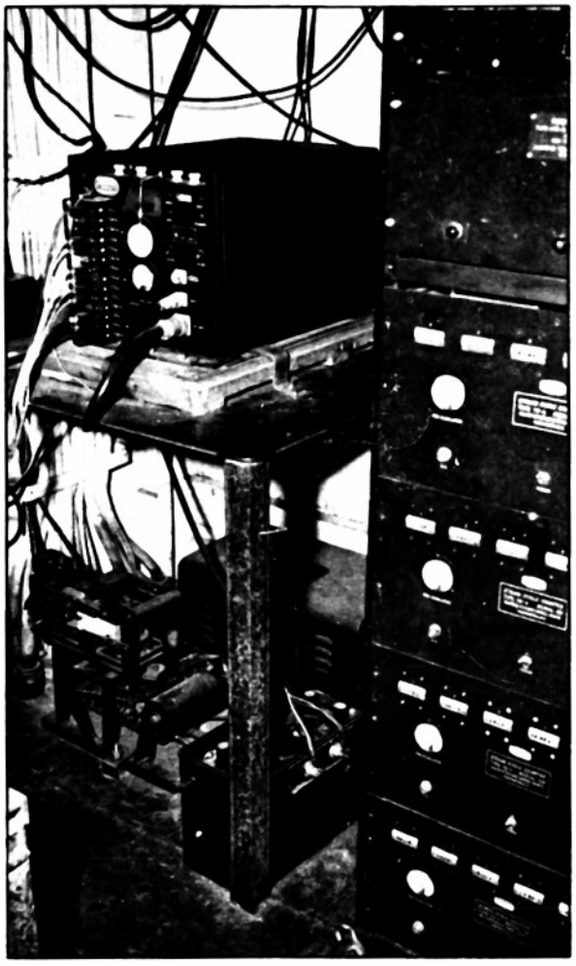

Figure 8 - Photograph Showing Installation of Strain-Cycle Counters, Pallograph, and Consolidated Oscillograph

Section B-B of Figure 4.

The general procedure during the tests was as follows: The ship's motion recorders were set to record for periods of 2 min. at 1-hr intervals. Oscillograph records of strain and pressure variation were taken at random intervals or whenever there appeared to be a noticeable change in the response of the ship to the sea; in addition, a record was taken every evening simultaneously with a record of the motion recorder. An average of three oscillograms was obtained each day. A photograph of the counter readings, similar to Figure 7, was taken every evening. The strain-cycle counters and the time totalizers were photographed at regular intervals of time. The difference of the readings between successive photographs gives the number of strain variations that have occurred within the corresponding interval. Occasional vibration measurements were made by means of the TMB Pallograph.[6] Wind and wave

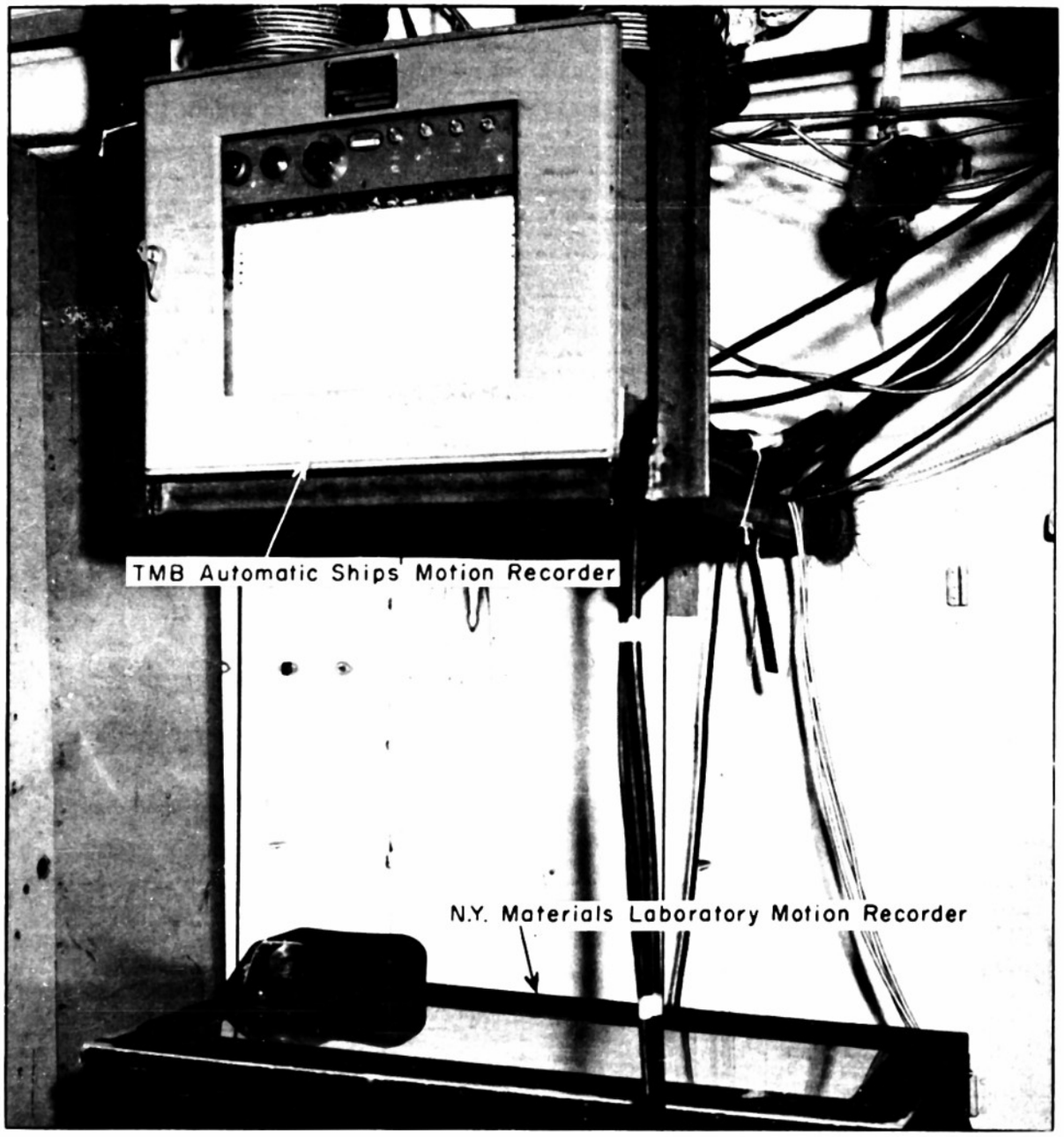

Figure 9 - Photograph Showing Installation of TMB Automatic Ship's Motion Recorder and of the New York Material Laboratory Ship's Motion Recorder

Section C-C of Figure 4.

data were obtained from the professional weather observers who recorded their data at 3-hr intervals throughout the trials.

PRESENTATION OF DATA

All the time-base data were obtained from either the ship's motion recorders or from the Consolidated oscillograph records; typical records are reproduced in Figure 10. These

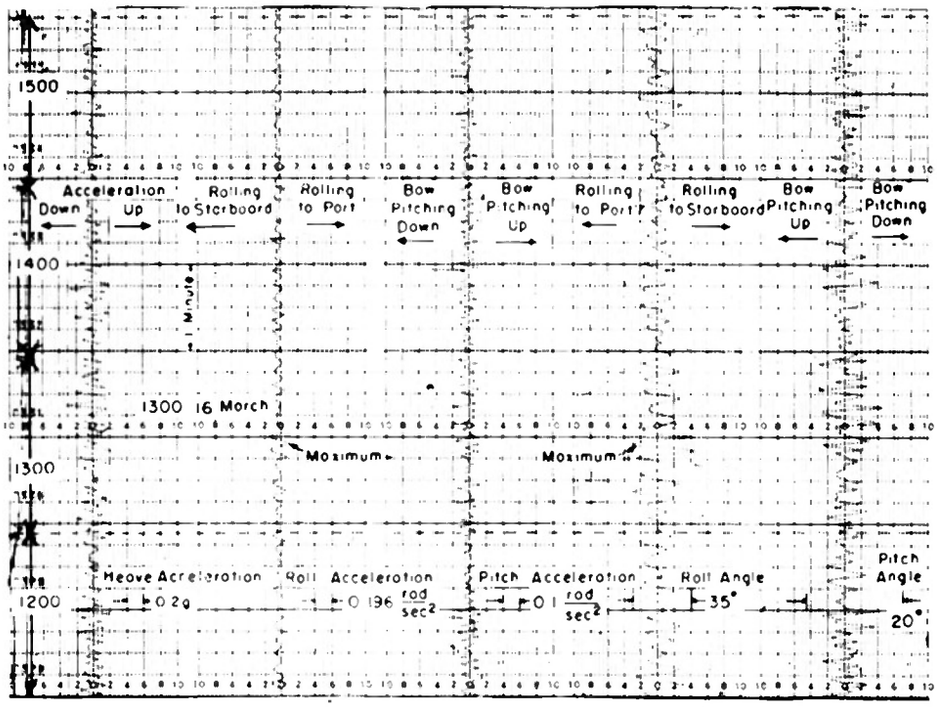

Figure 10a

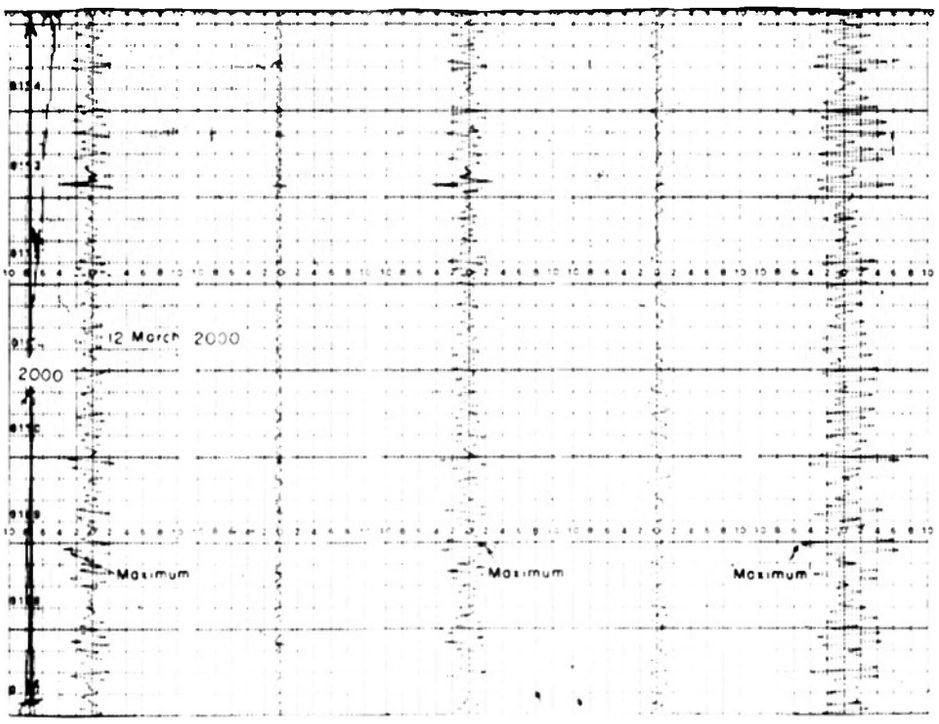

Figure 10b

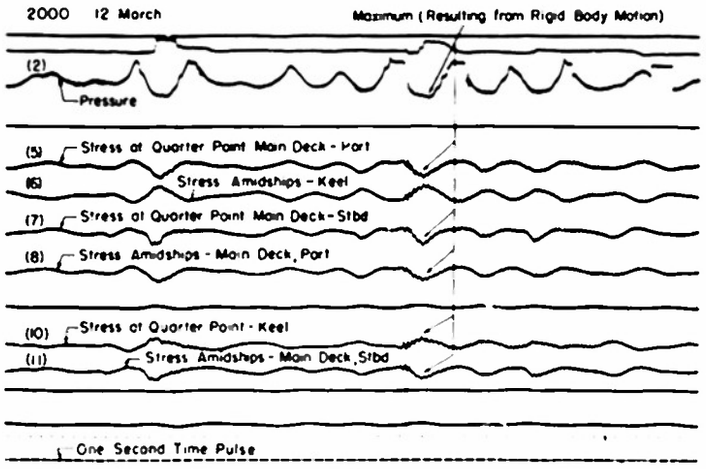

Figure 10c

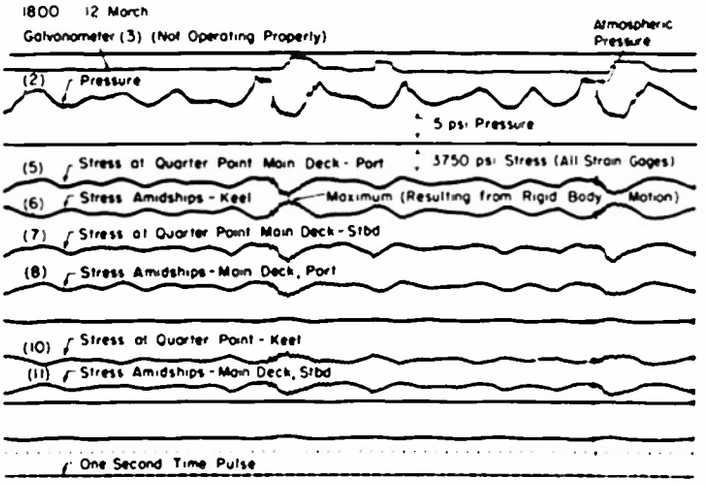

Figure 10d

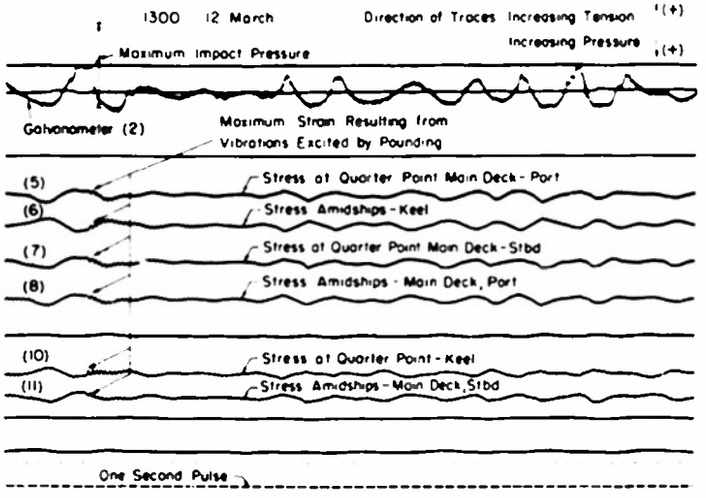

Figure 10e

Figure 10 - Oscillograms Recorded During the CASCO Trials, Indicating the Maximum Values Recorded Throughout the Trials

oscillograms were analyzed in terms of the number of positive and negative variations that had occurred in a given interval. A variation is here defined as the magnitude of the change in the measured quantity between a maximum and the succeeding minimum and vice versa; see Figure 11. This quantity, rather than the amplitude, was adopted for the sake of expediency because, in general, successive cycles did not have the same amplitude and because the mean level about which the variations occurred differed to some extent. A positive variation is de-

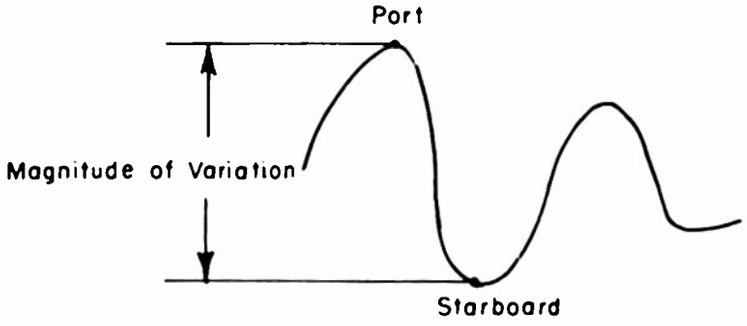

Figure 11 - Definition of Variation

fined as a variation in the positive direction. For example, positive heaving acceleration was defined as an acceleration in the direction of gravity; thus a positive variation in heave denotes an acceleration in the downward direction. It will be shown later that, in the over-all analysis, there will be about an equal number of positive and negative variations. Therefore to obtain the total number of cycles it will be nearly correct to add the positive and negative variations and divide this sum by two.

In order to present an over-all picture of the environmental conditions encountered and of the ship's response thereto, a number of quantities are plotted against time (Figure 12) for the entire duration of the voyage. The method of reporting weather and wave conditions used by the weather observers is given in Reference 7.

The TMB automatic ship's motion recorder[8] recorded data at hourly intervals for a duration of 2 min. These data were analyzed in terms of the number of variations that had occurred; the result of this analysis is given in Figure 13. To shorten the time required for data analysis, one 24-hr period was selected and an analysis was made of the heave accelerations measured during this period utilizing every sample, every second sample, third sample, fourth sample, etc. in an attempt to find the greatest sampling interval which would give about the same distribution pattern as would be obtained with hourly samples. It was found sufficient for the purpose here to analyze every third sample. For the heave acceleration (Figure 13e), all samples were utilized. For the other quantities every third sample was used. Each of the amplitude-frequency distribution curves (Figure 13) gives the total sampling time as well as the maximum value that was measured at any time throughout the tests. These maximum values are also tabulated in Table 2 together with the simultaneous values of the other measured quantities.

(Text continued on page 17.)

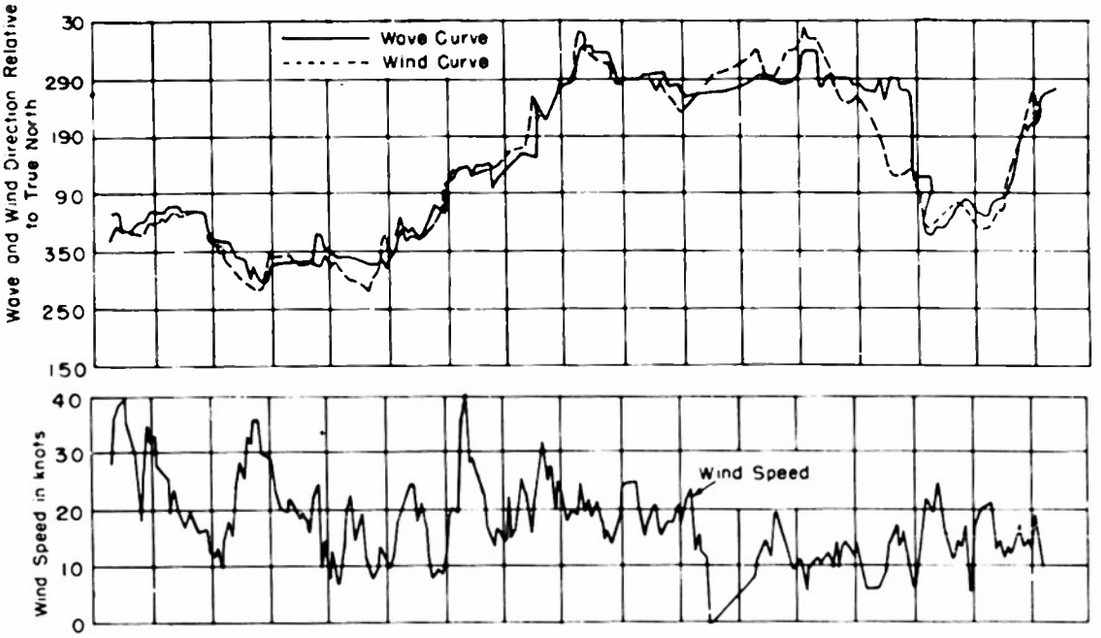

Figure 12a

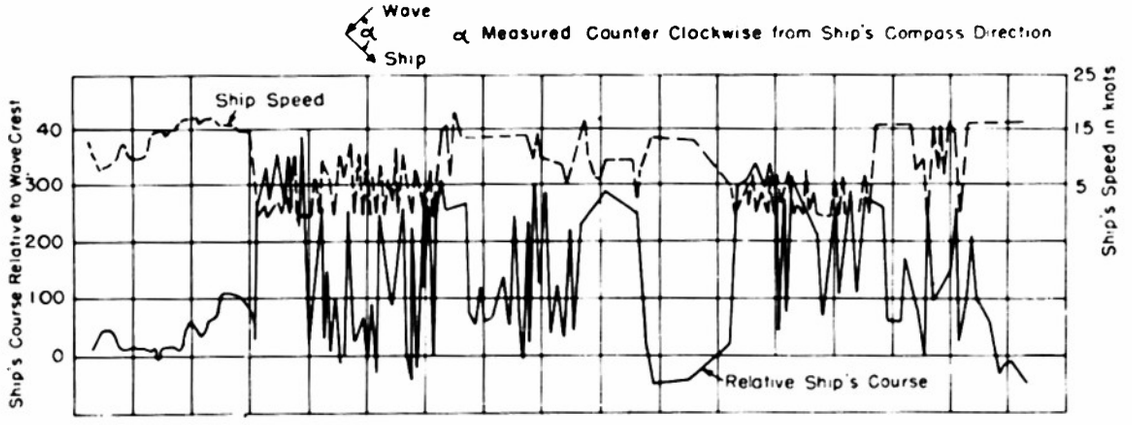

Figure 12b

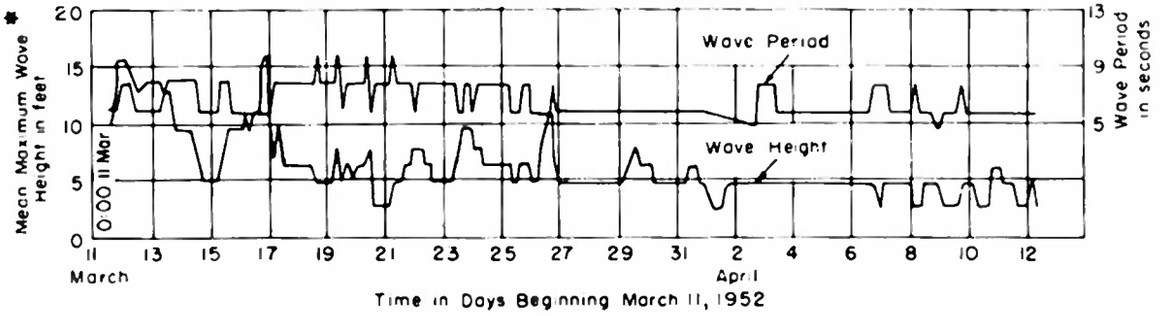

Figure 12c

* The mean maximum wave height is the mean of the maximum height of 15 to 20 well-defined waves, see Reference 7. Wave height is difference in level between crest and trough.

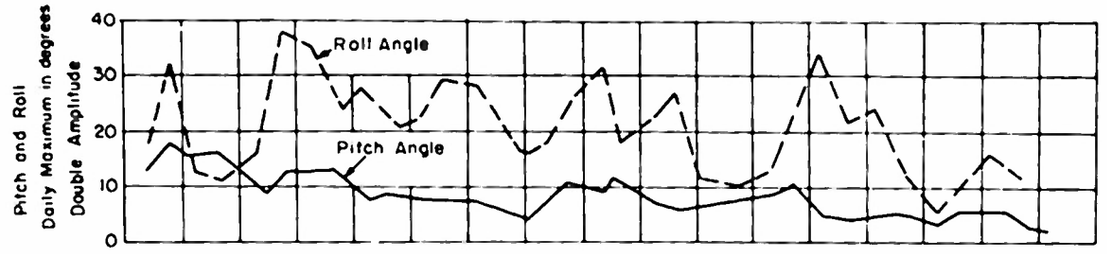

Figure 12d

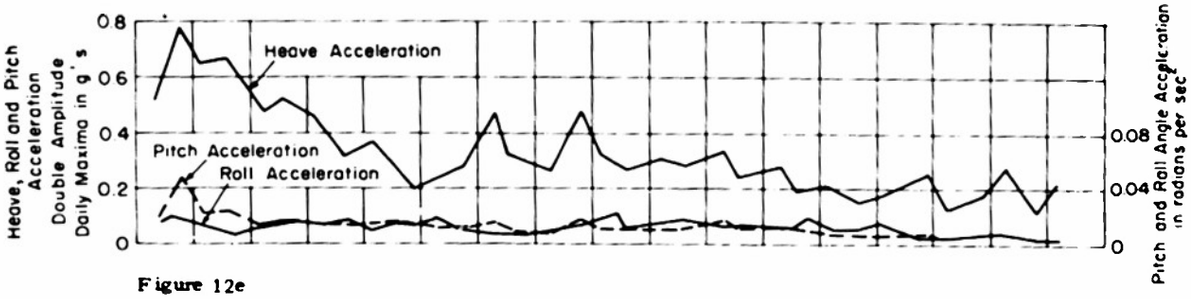

Figure 12e

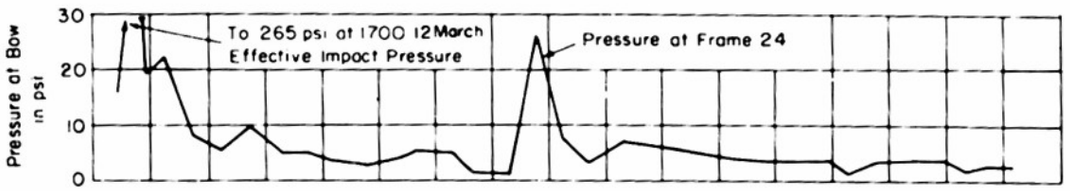

Figure 12f

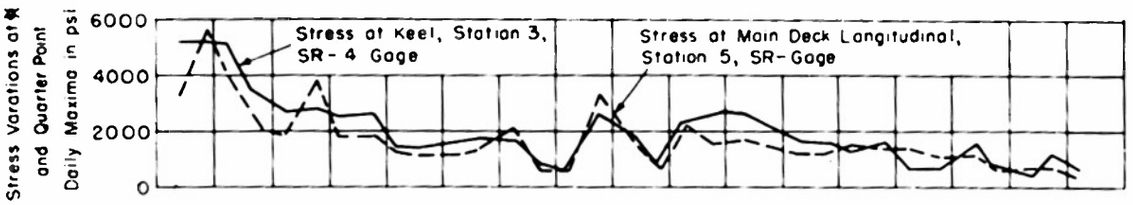

Figure 12g

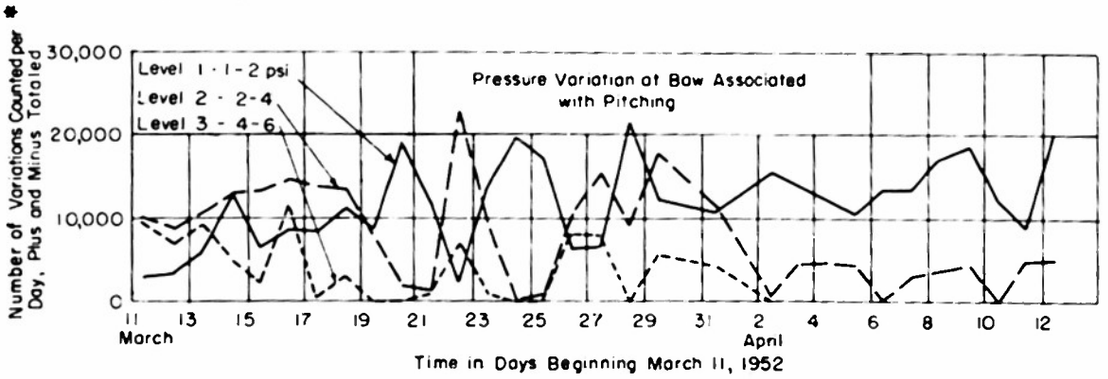

Figure 12h

*Total number of variations (including both negative and positive variations).

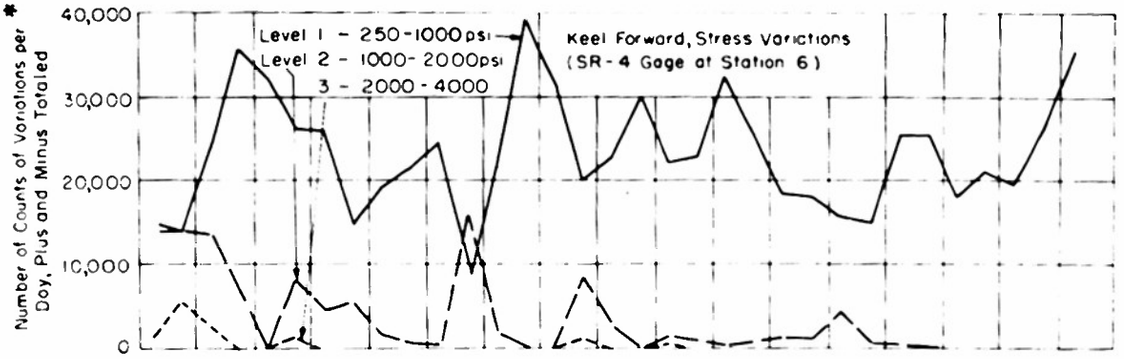

Figure 12i

*Total number of variations (including both negative and positive variations).

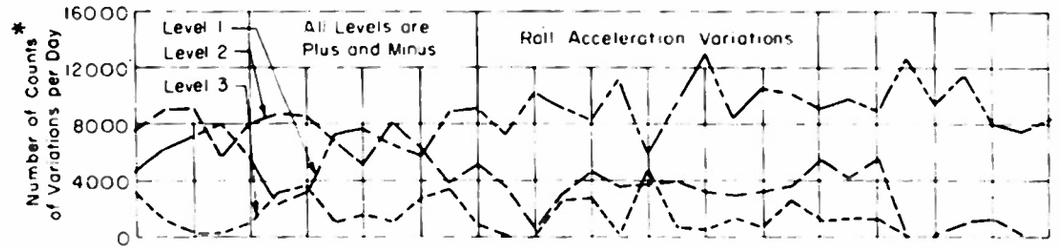

Figure 12j

* Total number of variations (including both negative and positive variations).

The magnitudes associated with these levels are given in Figure 13.

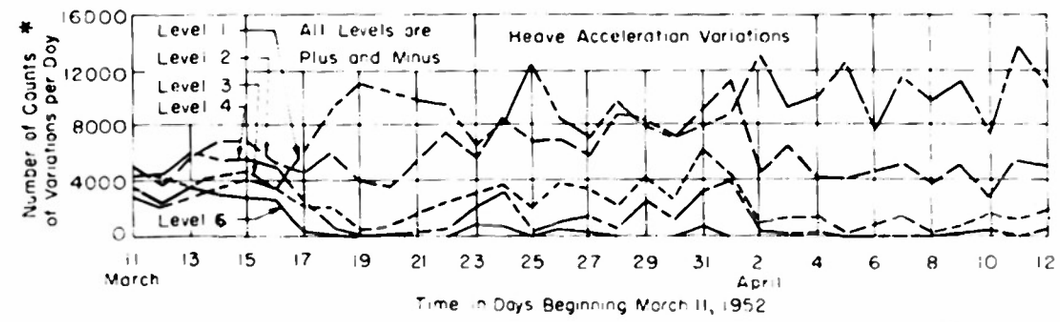

Figure 12k

*Total number of variations (including both negative and positive variations).

The magnitudes associated with these levels are given in Figure 13.

Figure 12 - Ship Motions, Stresses, and Environmental Conditions Plotted against Time

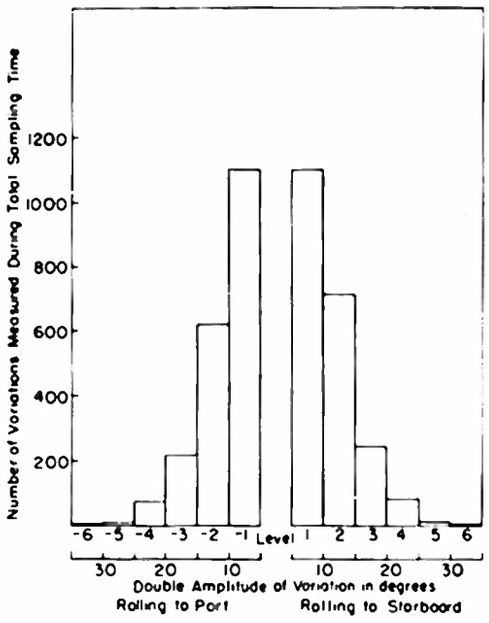

Figure 13a - Roll Angle

Maximum observed value: 15.5 deg. to port, 22 deg. to starboard; total roll 37.5 deg. Time of maximum observed value: 1300, 16 March 1951. Total sampling time: 29040 sec. Test period: 30 days.

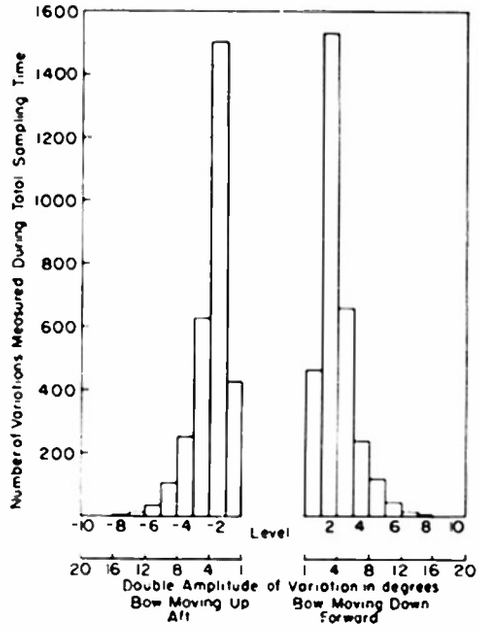

Figure 13b - Pitch Angle

Maximum observed value: 20.4 deg. double amplitude. Time of maximum observed value: 2000, 12 March 1951. Total sampling time: 29040 sec. Test period: 30 days.

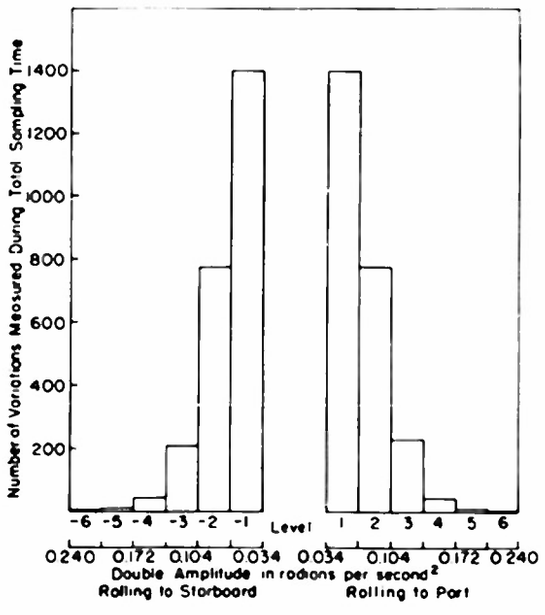

Figure 13c - Roll Acceleration

Maximum observed value: 0.26 rad/sec^2 double amplitude. Time of maximum observed value: 1300, 16 March 1951. Total sampling time: 29040 sec. Test period: 30 days.

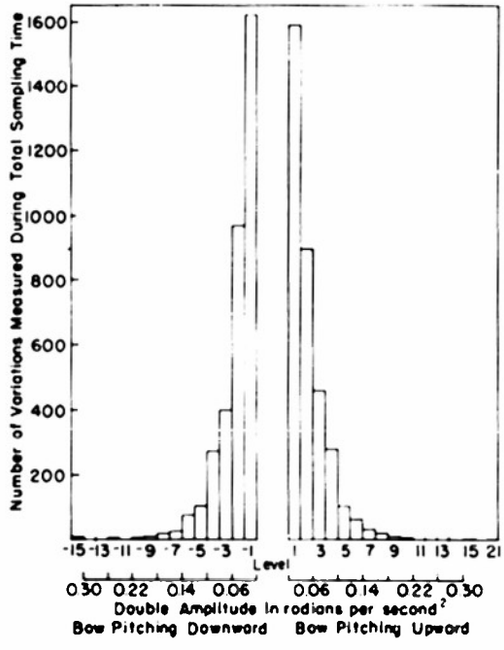

Figure 13d - Pitch Acceleration

Maximum observed value: 0.254 rad/sec^2 double amplitude. Time of maximum observed value: 2000, 12 March 1951. Total sampling time: 29040 sec. Test period: 30 days.

Figure 13e - Heave Acceleration

Maximum observed value: 0.51 g double amplitude. Time of maximum observed value: 2000, 12 March 1951 Total sampling time: 91080 sec. Test period: 30 days.

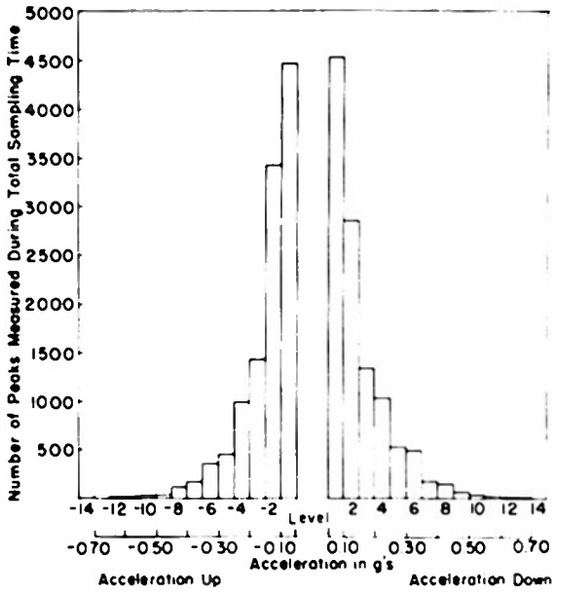

Figure 13 - Frequency Distribution of Roll, Pitch, and Heave

This figure gives the number of variations of given amplitudes that were measured throughout the total time during which measurements were made (sampling time). The number of total cycles of motion may be obtained by dividing the number of variations by two.

The ship-motion data were examined further to study the feasibility of presenting such data in terms of probability curves. It was found possible to do so; Figure 27 of Appendix 4 gives the resulting curves.

Sample oscillograms are shown in Figure 10. These oscillograms were obtained under some of the more severe conditions that were encountered; they will be discussed in the next section.

The data obtained by the strain-cycle counters are given in Figures 28 and 29 of Appendix 4; Figure 28 gives the cumulative counts whereas the incremental counts made each day are shown in Figure 29.

DISCUSSION AND EVALUATION OF DATA

Although the motions of a ship and the strains in the ship are related to each other, it will be of advantage here to discuss these two types of data separately and then perhaps to examine their relationships.

SHIP MOTIONS

Examination of the motion records obtained with the TMB automatic ship's motion recorder permits the following rather general observations.

TABLE 2

Significant Values Measured* on USCGC CASCO

Type of Variation	Quantity / Reference Oscillogram	Date and Time**	Recorded on TMB Automatic Ship's Motion Recorder					Recorded on Consolidated String Oscillograph						
									Stress at Quarterpoint			Stress Amidships		
			Roll Angle degrees	Roll Acceleration rad/sec^2	Pitch Angle degrees	Pitch Acceleration rad/sec^2	Heave Acceleration g	Pressure Station 7 psi	Keel Station 6 psi	Main Deck Port Station 4 psi	Main Deck Starboard Station 5 psi	Keel Station 3 psi	Main Deck Port Station 2 psi	Main Deck Starboard Station 1 psi
Variations Resulting from Rigid Body Motions	Figure 10a	16 Mar 51 1300	(–37.5)	(+0.26)	5.8	0.086	0.33							
	Figure 10b	12 Mar 51 2000	2.5	0.04	(–20.4)	(+0.254)	(+0.51)							
	Figure 10d	12 Mar 51 1800						(+11.1)	(2600)	(4700)	(3800)	(4700)	(3700)	(3100)
Variations Resulting from Vibrations Excited by Slamming	Figure 10e	12 Mar 51 1300						(>15) See Note	1400	790	1020	1120	840	750

**See Figure 10 for copies of the actual records.

Note: Slamming of the ship between 1600 and 1740 on 12 March caused a permanent deformation of the pressure gage diaphragm. Calculations of the pressure necessary to cause this deformation indicate that the pressure was about 265 psi.

*All values represent double amplitudes; numbers in parentheses are the maximum values measured throughout the tests. Data listed on the same horizontal line are for simultaneous measurements.

a. The heaving and pitching motions appear to be closely related when the sea is relatively rough; under these conditions the oscillograms are similar, and the periodicity of these motions is generally about the same. Under certain sea conditions (for example at 1900 and 2200 on 26 March) the time-variation pattern of the pitching angle appears quite different from the time-variation pattern of heaving acceleration although the pitching-acceleration and heaving-acceleration oscillograms still indicate similar frequency content.

b. The time interval between successive rolls, as taken from the record of roll angle, varied from 8.6 to 12 sec throughout the trials, with most of the rolls varying between 10 and 12 sec. The computed natural period[9] is 10.8 sec. It appears, therefore, that the rolling period of this ship did not depart greatly from the natural period of rolling.

The time interval between successive pitching motions, as taken from the records of pitch angle, varied from 4.6 to 20 sec for the time covered by the sea trials. An approximate computation gave a natural pitching period of 5 sec. Although most of the measured pitching motions were associated with periods from 4.5 to 6 sec, fairly steady pitching motions of much longer periods were encountered occasionally. The average wave periods, as estimated by the weather observers, ranged from 5 to 10 sec; see Figure 12c. The ship's course relative to the waves varied over a wide range, as indicated in Figure 12b, and therefore the "apparent wave period" also covered a wide range. It may be inferred that the ship's pitching period is greatly influenced by the "apparent period" of the waves. In short, the ship tended to roll at a period close to its natural period of roll but to pitch at the period of the forcing moments.

c. The time interval between successive peaks of heaving acceleration was from 4.2 to 7.5 sec. However, if this acceleration signal were integrated twice to give the heaving displacement, then the resulting displacement probably would show the same general pattern of time variations as the record of angular pitching displacement. The natural heaving period was computed to be approximately 5.3 sec.

d. In general, it was found that when the pitching motion was large, the heaving motion was also large (although their maxima do not generally occur simultaneously) but the roll was relatively less severe. On the other hand, when the rolling motion was quite severe, the heaving and pitching motions were not very large. The probability is that the most severe pitching and rolling motions will not occur simultaneously, and for design purposes, simultaneous maximum values of these quantities need not be assumed.

The following comments concerning the transducers are in order. The individual linear accelerometers measure accelerations perpendicular to their bases, and, if the ship rolls, the heaving acceleration measured is the component parallel to the instantaneous centerline plane of the ship. The heave accelerometer will also be affected by the change in the component of gravity along its sensitive axis. The error due to the latter cause is generally not serious except for the larger angles of roll; for the largest measured rolling angle (17.7 deg. single

amplitude) this effect would give an apparent heave acceleration of 0.05 g which, in this case, amounted to an error of about 20 percent in the measured heave-acceleration signal. The importance of this type of error is minimized by the observation made in (d) preceding, namely, that the most severe heaving and rolling motions will probably not occur simultaneously. If desired, correction for such effects can readily be made, provided that the oscillogram is available. In measuring angular accelerations, the effects due to the change in the gravity field or due to linear accelerations are canceled out.

An inspection of the frequency distribution of the cyclic variations in ship motions, Figures 13a to 13e, shows that in each case there are nearly as many positive variations of a given magnitude as there are negative variations. The data given in these figures have also been further analyzed in order to study the feasibility of presenting such data in terms of probability curves. It was found that the ship motion data did fall into a normal (Gaussian) distribution pattern; see Figure 27 in Appendix 4.

The presentation of data in the form of probability curves, as in Appendix 4, lends itself readily to engineering applications. For example, if it were desired to design some piece of equipment to operate properly for 95 percent of the time at sea and if the angle of pitch were a salient characteristic in the design requirements, then from Figure 27 of Appendix 4 it can be seen at once that 95 percent of the time the angle of pitch will be less than 7.6 deg. Of course, the curves given here are valid only for the particular conditions and type of ship from which they were derived. A great mass of similar data covering a wide variety of sea conditions and ship types would need to be obtained in order to cover the various possible combinations that would be of interest. However, if the distribution pattern is found to hold generally, this type of statistical presentation does give the required salient information in a concise manner from a mass of data. Automatic counting and tabulating devices reduce the labor required in collecting and analyzing such data sufficiently to make its utilization practical.

WIND AND WAVES

It was found, during these tests, that the direction of wind and waves coincided fairly well; see Figure 12a. All weather and wave data were obtained from the official weather observers stationed on the CASCO. In order to obtain some estimate of the length and velocity of the waves, the following Rankine[10] formulas for waves in deep water will be applied to the estimated wave periods plotted in Figure 12c.

$$\text{Length of the Wave, } L = 5.12\ T^2 \text{ ft, and}$$

$$\text{Velocity of the Wave, } V = 5.12\ T \text{ ft/sec}$$

where T is the period of the wave in seconds. The wave period varied from 5 to 10 sec; therefore the estimated value of L would range from 128 to 512 ft and that of V would range from 25.5 to 51.2 ft/sec.

The maximum wave heights of 16 ft, observed on 11 March, corresponded to an estimated period of about 8 sec; for these waves, Rankine's formulas give $L = 330$ ft and $V = 41$ ft/sec. The heading of the ship relative to the wave crest was 50 deg. at this time; therefore the apparent length of the wave was about 330/cos 50 deg. = 510 ft. If the ship had been headed directly into the waves, the stressing of the hull girder would have been much more severe since the length of the wave (330 ft) would then have been nearly equal to the length of the ship (300 ft).

HULL STRESSES AND PRESSURES

On 12 March between 1800 and 2000, the hull stresses, pitching motions, and heaving motions were the most severe recorded during the entire trip (see Table 2 and Figure 10). At this time the wave period varied from about 5 to 7 sec, the "mean maximum"[7] wave heights were about 14 ft, and the ship's course relative to the wavefronts was about 15 degrees, that is, the vessel was almost directly headed into the waves. Application of Rankine's formulas yields apparent wavelengths from 130 to 260 ft and wave velocities from 25 to 36 ft/sec. The length of the CASCO is 300 ft between perpendiculars, and it is therefore probable that the maximum stresses were realized with a wavelength which approached the length of the ship.

The largest strain and pressure variations recorded throughout the tests are listed in Table 2. The corresponding oscillograms, shown in Figures 10c, d, and e, are typical of the pattern usually recorded. Inspection of the oscillograms shows that the stresses associated with the rigid-body motions of the ship are much larger than the higher frequency stress variations due to flexural vibration of the hull subsequent to slamming of the bow. They also show that the pressure recorded by the pressure gage at the bow does on occasion indicate atmospheric pressure (a flat top on the galvanometer trace), evidence that the ship's bottom has come clear of the water as in the photograph shown in the frontispiece; this is followed by a very large pressure variation due to impact between the ship's bottom and the oncoming wave. The rapid pressure variations at the beginning of the impact are quite large and on occasion do include an initial negative pressure (cavitation) approaching an absolute vacuum. Subsequent to the impact, a flexural vertical vibration of the ship in its fundamental mode occurs as indicated by the higher frequency strains superimposed on the slower normal strain variations. This flexural vibration could also be distinctly felt as a "shudder" running through the ship subsequent to the slamming of the bow against the sea.

The frequency of this flexural vibration, as indicated by strain and vibration measurements, was about 150 cpm. The computed natural frequency of vertical flexural hull vibration for this ship, neglecting the rigidity of the superstructure, is 120 cpm for the two-noded mode of vibration. It will be shown later that the rigidity of the superstructure should not be neglected.

The diaphragm of the pressure gage was subjected to a permanent set in the interval between 1600 and 1740 on 12 March, due to large pressures caused by slamming. This "set" caused a large shift in the zero position of its galvanometer trace; however, the gage performed satisfactorily for the remainder of the trials and furnished much additional valuable data. It was necessary to recalibrate the gage after returning to the laboratory and to utilize the new calibration, which gave about half the sensitivity of the original calibration, for the portion of the data obtained after the permanent set had occurred. The gage had been designed and calibrated with statically applied pressures up to 100 psi. Approximate calculations, based on the theory of plasticity[11] and the known permanent set of the diaphragm, indicate that the effective static pressure causing the measured set of the diaphragm was in excess of 265 psi.* The ruptures of bottom-plating panels that have occurred in the region in which the pressure gage was located are, no doubt, due to the large pressures incident to slamming action in a seaway. It is interesting to note that relatively large hull stresses were measured at the same time that slamming was prevalent.

It was stated previously that strain measurements were made by means of the strain-cycle counters as well as by oscillographic recording of strain variations. In order to present the strain data in a compact form useful for evaluating the fatigue strength requirements of ship hulls, the strain variations counted by the strain-cycle counters have been presented as cumulative counts for each day as well as in terms of the number of counts made each day; see Figures 28 and 29 of Appendix 4. The data for the 4000- to 8000-psi range show a large discrepancy between the number of variations measured by the two adjacent gages. The explanation is simple. The accuracy of setting the strain-cycle gage was within about 300 psi; therefore the indication is that the difference in the number of counts registered by the two gages represents cyclic variations of a magnitude very nearly equal to the lower limit of the corresponding range. For example, in Figure 28b of Appendix 4 most of the variations indicated by Counter 101 were about 4000 $\pm$ 300 psi and, at the most, 13 1/2 cycles of about 8000 psi could have occurred throughout the trials.

Similar graphs of occurrence rates for the number of cyclic variations of stresses, pressures, and motions, as derived from the oscillograph and ship-motion-recorder records, are shown in Figures 12h, i, j, and k. Inasmuch as some of the occurrence rates are based on a very limited number of samples, little reliance can be placed on the values given. However, the data give some idea of the order of magnitude involved. It can be concluded from these analytical data that endurance strength may need to be considered in the longitudinal strength design of ships.

The strain data indicate that the mean level of strain remains nearly constant. The change of mean strain level due to change in loading can be computed fairly readily, and it is therefore concluded that for shipboard measurement it will be sufficient to classify strain

*Pressures of this magnitude must be of relatively short duration and extend over very limited area of plating.

variations according to the magnitude of the variation only, that is, the additional automatic classification by mean strain level may be omitted.

Figures 12e, f, and g give the peak values of (a) stresses measured by the SR-4 gages at Station 5 (main-deck longitudinal near ship's forward quarterpoint) and Station 3 (keel, Frame 61), (b) pressure at the bow, and (c) rolling, heaving, and pitching accelerations for every day of the trials. The plots for heave acceleration, pressure, and stresses show a strong resemblance to one another.

Examination of the maximum stress variations measured (see Table 2) show that the actual magnitudes were not great, i.e., 4700 psi associated with the rigid-body motion of the ship and 1400 psi associated with the flexural vibration of the ship subsequent to slamming. It was noted from inspection of the data in Table 2 that the ratio of stress in the main-deck longitudinal to that in the keel, measured near the forward quarterpoint of the ship (Frame 41), was substantially different for the vibratory stresses subsequent to slamming than for those stresses due to the rigid-body motion of the ship. This indicates nonlinear strain variation of the hull when subject to slamming. This fact is of considerable interest and is discussed in Appendix 2. Although the tests were not arranged to study this particular phenomenon; nevertheless, it seems advisable to call attention to this observation. It should be remembered that the alternating stresses associated with the flexural vibration due to slamming, although of a low order of magnitude (about 1400 psi), are nevertheless many times the stresses incident to ordinary hull flexural vibrations.

It was of interest to determine the position of the neutral axis in longitudinal bending of the hull, for both hog and sag conditions, on the basis of the strain measurements as recorded by the Consolidated oscillograph (strains associated with the rigid-body motions of the ship). For this purpose a number of simultaneous stress measurements were analyzed covering the range from about 1000 to 5000 psi, double amplitude. The results of this analysis are shown in Figure 14. It is readily apparent that over the range of stresses available for study, the position of the neutral axis at Frame 61 remains sensibly fixed in the ship for both hog and sag conditions of loading. The position of the neutral axis at Frame 41 was more difficult to check, probably due to the rather low magnitude of the low-frequency strain variations at the keel. Comparison of the position of the neutral axis as computed from plans with that computed on the basis of strain measurements indicates that the superstructure contributes appreciably to the longitudinal bending rigidity of the hull. This is discussed further in Appendix 1.

EVALUATION OF HULL STRENGTH CALCULATIONS

An attempt will be made in this section to explain why the magnitudes of the measured hull girder stresses were relatively so small when the static strength calculations would lead one to expect much larger values. The lack of agreement of the stress distribution at Frame 41,

Computed Location of Neutral Axis and Section Moment of Inertia				
	Distance of Neutral Axis from Base Line		Moment of Inertia about Neutral Axis	
	By TMB	By PSNY*	By TMB	By PSNY*
Frame 57, with deckhouse	13.8 ft	-	761 ft^4	-
Frame 57, without deckhouse	11.2 ft	10.9 ft	499 ft^4	376 ft^4
Frame 40, without deckhouse	12.9 ft	12.3 ft	380 ft^4	321 ft^4
Frame 40, with deckhouse	15.5 ft	-	596 ft^4	-

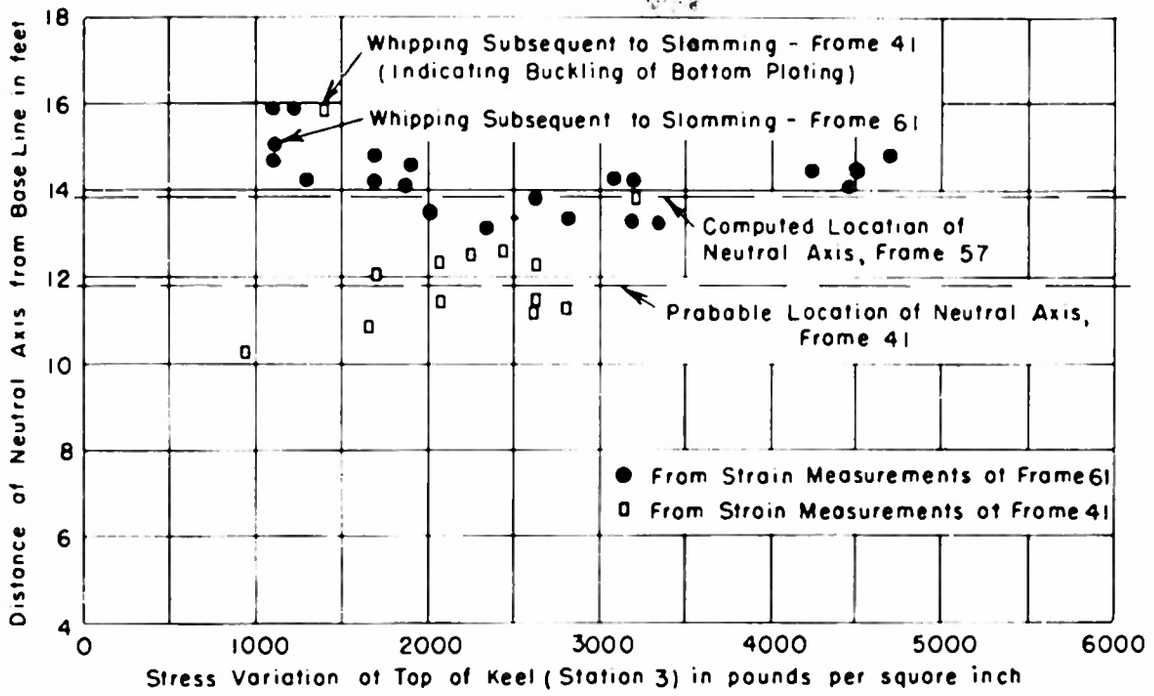

*Puget Sound Naval Shipyard Plans used: AVP 1011-2907-2, AVP 1011-2907-3, and AVP 1013-1111-2.

Figure 14 - Location of Neutral Axis

under conditions of slamming, with that expected according to simple beam theory will also be touched upon.

The largest strains and hull motions were measured between 1800 and 2000 on 12 March; see pages 10 and 11. The waves which gage rise to these stresses were estimated to be 260 ft long and 14 ft high.[7] It is reasonable to assume that the maximum measured heave and pitch motions as well as the maximum hull strains occurred during the passage of a single large wave.* Inspection of the sample oscillograms, Figure 10, shows that there are a number of large cyclic variations of stresses and motions in a relatively short span of time and that their peak values do not differ greatly. The assumption will therefore be made that the maximum measured values of heave and pitch accelerations and hull strains occurred while the ship passed through a wave 260 ft long and 14 ft high. Figure 15 shows the bending moment and shear

*The assumption is supported by the fact that the maximum measured pitch angle during the same time interval was about 20 deg. as compared with a computed pitch angle of 16 1/3 deg. double amplitude for Case 8 combined with Case 6, Table 3.

TABLE 3

Computed Hull Girder Loading for a Number of Selected Attitudes of Ship and Wave

	Assumed Condition of Ship on Wave*	Angle between Line of Centers of Rolling Circle and Keel**	Bending Moment M, ft-tons Shear V, tons Flexural Stress σ, psi***	Bending Moment, Shear, and Stresses						Midships	Maximum Value	Location of Maximum ft from bow
				Frame 40	Frame 41	Frame 42	Frame 57	Frame 61	Frame 71.5			
				Section Modulus Used was Computed at Frame 40 (without deckhouse) see Figure 14.			Section Modulus Used was Computed at Frame 57 (with deckhouse) see Figure 14.					
1	Still Water Zero Acceleration (Static)	0 deg. - 0 min.	M	-2800	-2900	-3000	-4500	-4900	-5200	-5100	-5200	114.8
			V	46	39	33	66	45	-17	-23	72 -96	102.5 190.7
			σ Main Deck		+1660			+1140	+1210			
			σ Keel		-1410			-1390	-1470			
2	Sag Bow Up Zero Acceleration (Static)	1 deg. - 40 min.	M	4200	4800	5200	11,600	13,200	16,200	16,900	17,000	157
			V	-190	-208	-218	-186	-168	-107	-55	-235 303	95 225
			σ Main Deck		-2740			3050	-3760			
			σ Keel		+2320			+3750	+4580			
3	Hog Bow Down Zero Acceleration (Static)	2 deg. - 10 min.	M	-8900	-9200	-9700	-17,400	-19,300	-22,300	-22,500	-22,500	150
			V	250	250	248	269	227	51	13	288 -284	105 200
			σ Main Deck		+5250			+4480	+5170			
			σ Keel		4450			-5460	-6310			
4	Sagging Zero Trim	0 deg. - 0 min.	M	2900	3300	3700	10,800	12,600	17,600	19,100	21,300	172.5
			V	-171	-194	-213	-222	-226	-216	-170	-240 379	135 227
			σ Main Deck		-1880			-2920	-4080			
			σ Keel		+1600			+3560	+4980			
5	Sagging Bow Up	0 deg. - 55 min.	M	5700	6300	6800	15,400	17,700	22,800	24,200	25,600	169
			V	-245	-263	-278	-270	-267	-210	-160	-307 415	92 225
			σ Main Deck		-3600			-4100	-5290			
			σ Keel		+3050			+5000	+6450			
6	Sagging Bow Down	-3 deg. - 35 min.	M	5900	6300	6800	13,700	14,700	16,600	16,900	17,000	153
			V	-225	-245	-257	-140	-118	-35	10	-268 263	90 225
			σ Main Deck		-3600			-3410	-3850			
			σ Keel		+3050			+4150	+4700			
7	Hogging Zero Trim	0 deg. - 0 min.	M	-6600	-7000	-7400	-13,900	-16,000	-18,300	-18,600	-18,700	152
			V	196	198	199	230	195	68	+25	243 -253	109 201
			σ Main Deck		+4000			+3700	+4250			
			σ Keel		-3390			-4530	-5180			
8	Hogging Bow Up	12 deg. - 45 min.	M	-1500	-1650	-1800	-6000	-7300	-10,200	-10,600	-10,800	163
			V	87	91	96	190	179	94	67	190 -150	113 200
			σ Main Deck		+940			+1690	+2370			
			σ Keel		-800			-2060	-2890			

Note: The shear and bending moment values are taken from Figure 15. The signs of M and V are taken in the conventional sense.

*The vessel is assumed to encounter a wave 260 ft long and 14 ft high. Unless otherwise noted the ship is assumed to have an instantaneous pitch acceleration of 0.125 rad/sec^2, a heave acceleration of 0.25 × gravity upward in sag and 0.35 × gravity downward in hog. These accelerations are the maximum accelerations measured.

**A trochoidal wave is assumed here. The line of centers refers to the locus of the center of the rolling circle generating the wave profile.

***The stress is computed at the main deck and the bottom of the keel. The location of the neutral axis is taken as 13.8 ft and 11.8 ft above the base line in Frames 61 and 41, respectively.

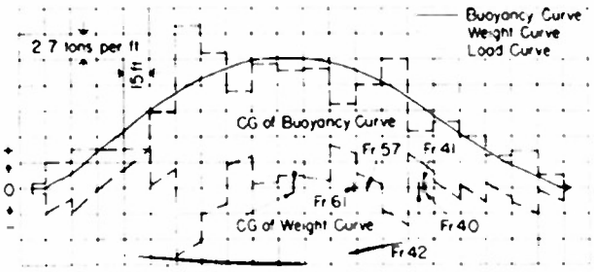

1. Still water, zero acceleration (static)

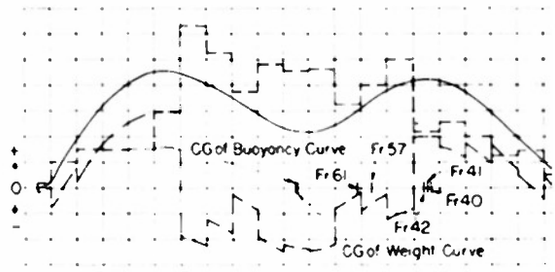

2. Sag bow up, zero acceleration (static)

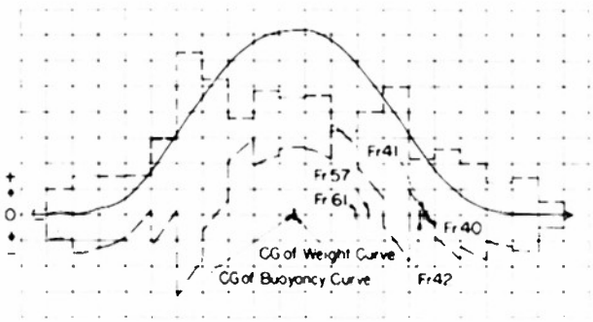

3. Hog bow down, zero acceleration (static)

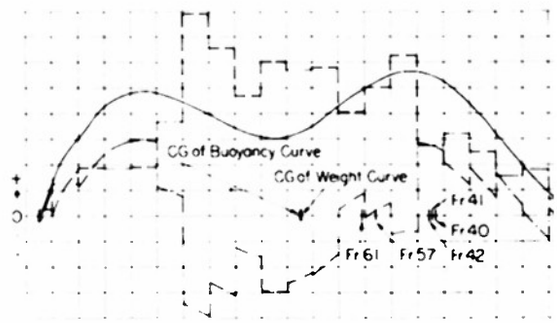

4. Sagging, zero trim

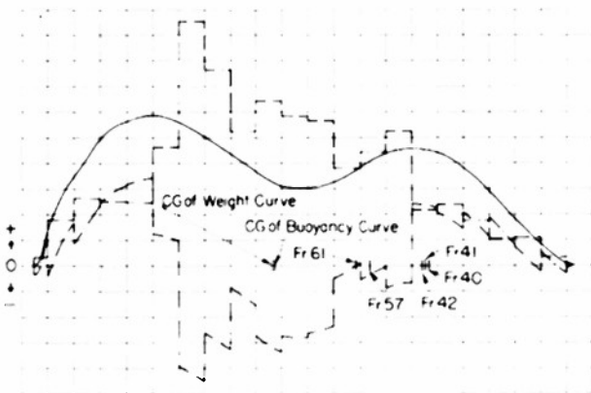

5. Sagging, bow up

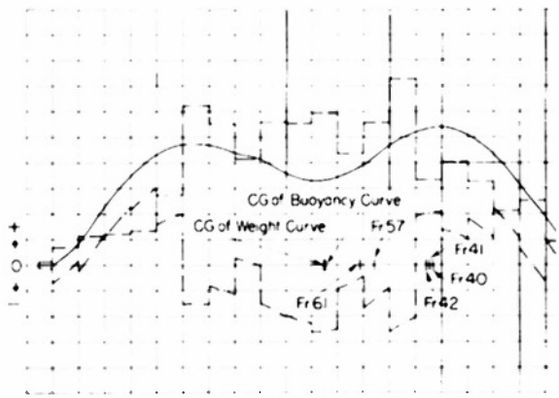

6. Sagging, bow down

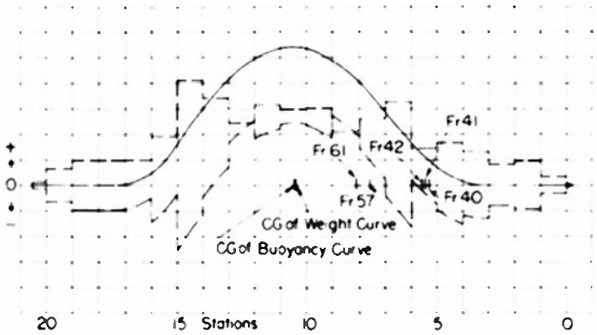

7. Hogging, zero trim

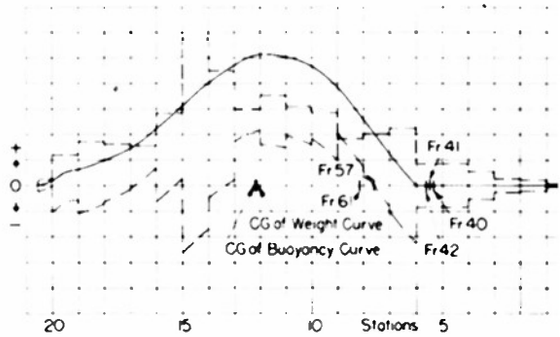

8. Hogging, bow up

15a - Weight, Load, and Buoyancy Curves - The Ship's Bow is Located at Station Zero

(The weight curve is a plot of the "effective" weight distribution as explained on page 28).

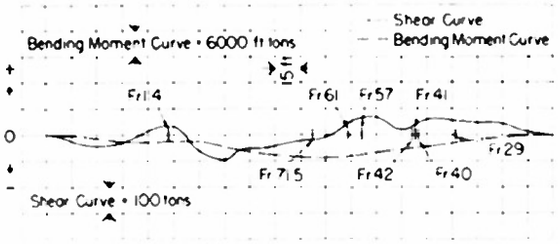

1. Still water, zero acceleration (static)

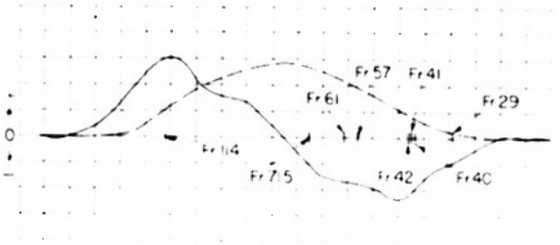

2. Sag bow up, zero acceleration (static)

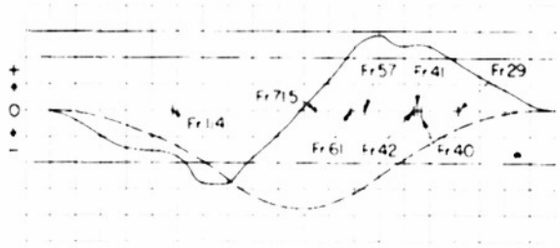

3. Hog bow down, zero acceleration (static)

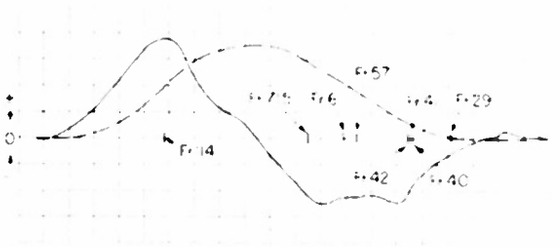

4. Sagging, zero trim

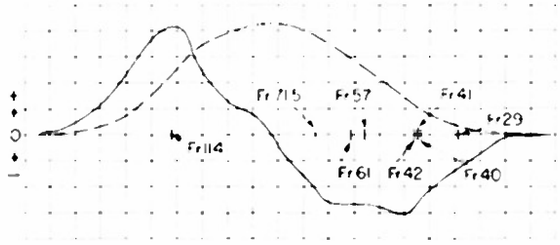

5. Sagging, bow up

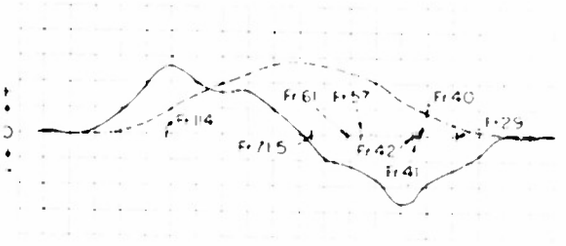

6. Sagging, bow down

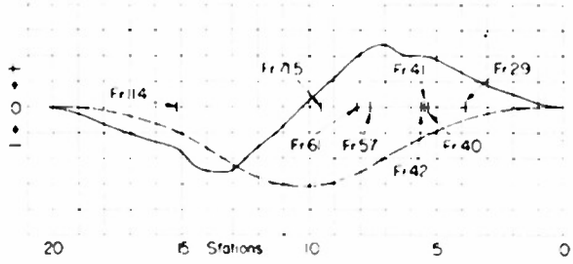

7. Hogging, zero trim

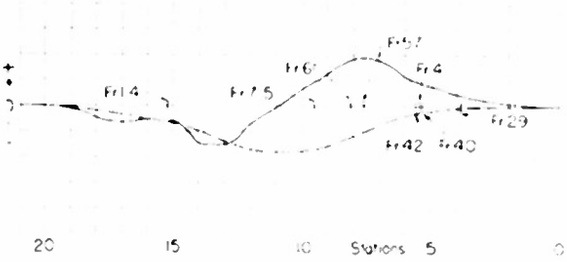

8. Hogging, bow up

Figure 15b - Shear and Bending Moment Curves - The Ship's Bow is Located at Station Zero

Figure 15 - Load, Shear and Bending Moment Curves for a Number of Assumed Positions of the Ship on a 260-Foot-Long, 14-Foot-High Wave

Weight curve is considered negative. All other curves + or − as plotted. See Table 3.

curves for the various possible combinations of the maximum heave and pitch motions. These curves were computed by a procedure designed to follow the standard strength calculation[12] as closely as practicable. The mathematical development of this procedure is given on pages 19 to 23 of Reference 13. The main steps are as follows:

a. An effective weight curve* is obtained for each case by multiplying the actual weight curve by the acceleration due to heave and pitch in gravity units (the direction of the acceleration is reversed according to d'Alembert's principle).

b. The ship is so oriented on the wave (260 ft long, 14 ft high) to satisfy the following equilibrium requirements:

1. The total effective weight must equal the total buoyant force.

2. The longitudinal position of the center of buoyancy must coincide with the longitudinal position of the center of area of the effective weight curve.

In addition to the various selected dynamic conditions listed in Table 3, the bending moment and shear curves were also computed** for the following reference positions:

1. With the ship in still water.

2. With the ship in the hog and sag conditions on a trochoidal wave 260 ft long and 14 ft high, using the standard procedure of assuming the ship to be in static equilibrium on the wave, i.e., neglecting all inertia effects.

The bending moments and shear forces thus computed at several selected longitudinal positions are taken from the curves of Figure 15 and are listed in Table 3. The strain measurements on the CASCO were made near Frames 41 and 61. The position of the neutral axis, based on the measured strains, was used to compute the hull girder stresses at Frames 41 and 61. The contribution to hull strength by the deckhouse was considered, as discussed in Appendix 1. It appears from a study of both ship strains and motions that, for the case of the maximum observed motions, the vessel is in a hogging position with the bow up followed by a downward motion of the bow as it meets the next oncoming wave. Therefore the combinations most likely to approximate actual conditions would be somewhere between Condition 8 together with 6 or Condition 8 together with 4, taken from Table 3. The computed stresses at the bottom of the keel and at the top of the main-deck longitudinals for these conditions are given in Table 3. A number of possible combinations of the conditions listed in Table 3 have been

---

*The weight distribution was taken from Reference 14. The actual displacement was 2460 tons at a mean draft of 12 ft 2½ in. as compared with a displacement of 2430 tons used in Reference 14.

**For the sake of convenience, the effect of the orbital motion of the water particles has been neglected in these strength calculations, that is, the wave has been considered to be a still mass of water. The effect of these orbital motions can be taken into account by means of the "Smith" correction; the result will be to reduce the value of the computed hull stresses by about 10 percent. It should be further noted that the effects of longitudinal forces due to wave resistance and propeller thrust have been neglected because, at this time, it does not seem feasible to evaluate these effects with reasonable accuracy. It is believed, however, that their contribution is not particularly significant.

given in Table 4 for comparison of computed and measured stresses. An examination of Table 4 indicates that the stress variations computed under consideration of the inertia effects are of the same order of magnitude as the measured values whereas the stresses computed with the usual assumption--that the vessel is statically poised on the wave--are considerably larger than the measured values. This is not meant to imply that the stresses under dynamic conditions are always less than for the usual static computation; however it does tend toward the conclusion, especially in the light of other full-scale sea tests, that for the conditions under which ships are operated the stresses are considerably less, as stated above. In Appendix 1

TABLE 4

Comparison of Measured and Computed Stress Variations

Combination	Total Stress Variation by Combining Two Conditions (Computed)*			Largest Measured Stress Variation	
	Conditions** Combined	Stress Change Top of Keel	Stress Change Bottom of Main Deck Longitudinal	Stress Top of Keel	Stress Bottom of Main Deck Longitudinal
8 and 4	8 and 4 At Frame 41 †	- 660 +1320 1980	+ 880 -1770 2650	2600	4200
8 and 6	8 and 6 At Frame 41 †	- 660 +2530 3190	+ 880 -3370 4250	2600	4200
8 and 4	8 and 4 At Frame 61†	-1730 +3000 4730	+1540 -2660 4200	4700	3400
8 and 6	8 and 6 At Frame 61†	-1730 +3490 5220	+1540 -3100 4640	4700	3400
8 and 4	8 and 4 At center of deckhouse	-2430 +4200 6630	+2150 -3720 5870	.	.
8 and 6	8 and 6 At center of deckhouse	-2430 +3960 6390	+2150 -3510 5660	.	.
2 and 3 Static	2 and 3 At Frame 41 †	+1930 -3700 5630	-2560 +4910 7470	2600	4200
2 and 3 Static	2 and 3 At Frame 61 †	+3140 -4600 7740	-2790 +4100 6890	4700	3400

*Stress distribution according to Bleich's method (Appendix 1) Deckhouse is neglected in way of Frame 41.

**As described in Table 3.

†Location of SR-4 strain gages.

the stress distribution in a section in way of the deckhouse is considered in more detail and measured and computed stresses are compared.

It would seem that an improvement over the present design procedure could be made along the lines utilized here if the maximum pitching and heaving accelerations that a given ship may experience were known. It is shown in Appendix 1 that a consideration of the contribution of the superstructure to the longitudinal hull girder strength according to the method suggested by H. Bleich[15] will result in a stress distribution and in magnitudes of stress much more nearly in agreement with the measured values than would obtain if the contribution of the superstructure were neglected. Although this method requires the use of a number of assumptions, it does indicate that the superstructure contributes materially to the girder strength and to this extent is in agreement with the measured strain data. Note also that the computed location of the neutral axis (13.8 ft above base line) in Figure 17a is in very good agreement with that given in Figure 14 for Frame 61.

The upward shift of the neutral axis noted at Frame 41 during slamming is probably due to elastic or plastic transverse deflection of the hull plating under combined axial and transverse loading which causes a redistribution of the load to the more rigid hull members; see Appendix 2. It seems possible that for some conditions buckling of the bottom plating could take place even though the hull girder stresses themselves are relatively low. The reduction in effective section modulus incident to local buckling of the bottom plating may, in turn, bring about a failure of the entire section, which to all appearances may look as though it were caused by excessive hull girder stresses.

CONCLUSIONS AND RECOMMENDATIONS

A. SHIP'S MOTION

1. The heaving and pitching motions of the ship had the same general pattern of time variation when these motions were large (in a relatively heavy sea).

2. The CASCO tended to roll with a period near its natural period of roll, but the indication is that the ship tended to pitch at the period of the forcing moments.

3. In general it was found that when the pitching motion of the ship was large, the heaving motion was also large (although the maxima of these motions did not generally occur simultaneously), but that the roll was relatively less severe for these conditions. On the other hand, when the rolling motion was quite severe, the heaving and pitching motions were not very large. In short, for a given ship in a given sea, it is improbable that the most severe pitching and rolling motions possible will occur simultaneously. For design purposes, simultaneous maximum values of these quantities need not be assumed.

4. It has been possible to present the ship's motion data in terms of normal distribution patterns; see Figure 27 of Appendix 4. The presentation of data in the form of probability curves readily lends itself to engineering applications and at the same time makes it

possible to give the required salient information, based on a mass of statistical data, in a concise convenient form.

5. The ship vibrated in the two-noded mode of vertical flexural vibration subsequent to each impact between the forward part of the ship's bottom and the sea.

6. The pressure due to the slamming action, measured during these tests, may cause large stresses in the bottom plating which is subjected, in addition, to the stresses due to longitudinal bending of the hull. It is believed that slamming of the bow against the sea does not, in itself, cause severe stressing of the hull girder but does cause severe loading of the local bottom structure. Failure of this local structure may initiate a subsequent failure of the hull girder.

7. It is recommended that automatic ship's motion recorders equipped with statistical analyzing and tabulating devices, such as are being developed at the Taylor Model Basin, be installed on a number of selected ship types in order to collect statistical strain and motion data similar to that shown in Figures 27 to 29 of Appendix 4.

B. HULL STRENGTH

On the basis of the discussions of the strain and pressure data, it is concluded that for the USCGC CASCO:

1. The stresses associated with the rigid-body motions of the hull are considerably larger in magnitude than the stresses due to flexural vibration of the hull incident to slamming, but they are much less than the static stresses computed for the ship poised on a wave of the same approximate dimensions as the wave producing the measured strains.

2. The longitudinal bending stresses near the forward quarterpoint of the hull are of the same order of magnitude as those near the midship section. The maximum values of the recorded stresses were small.

3. The simple-beam theory appears to apply to the hull girder for the low-frequency stress variations incident to rigid-body motion but its use is questionable for flexural vibratory stresses subsequent to slamming, on the basis of the meager evidence available here.

4. The pressures acting locally incident to slamming may reach very large instantaneous values and do on occasion reach negative values approaching a vacuum.

5. When conditions were such as to result in large hull stresses associated with the rigid-body motions of the ship, large vibratory stresses due to slamming were also observed.

6. In view of the large local loading indicated in the CASCO tests, it is suggested that the strength of the local bottom structure near the bow be given special attention in ship design, especially with regard to the effect on the over-all longitudinal girder strength.

7. The strain cycle gage data indicate that the endurance strength under repeated load needs to be considered in the strength design of ships.

APPENDIX 1

STRESS DISTRIBUTION IN WAY OF THE DECKHOUSE

Strains measured in way of the deckhouse structure† at Frame 61 gave a stress distribution and a location of the neutral axis which showed that the superstructure did contribute materially to the hull girder strength. The measured stresses and those computed according to the method outlined on page 28 for the conditions shown in Table 3, attain the same order of magnitude if the deckhouse, to the superstructure deck, is included in the computation of the section moment of inertia. The stresses measured in way of Frame 41, although rather low and consequently not very reliable indicate that the contribution of the deckhouse here, near its termination, is small.

A method has been proposed by H. Bleich[15] which permits evaluating the contribution of the ship's superstructure to the hull strength. It was decided to apply this theory to the CASCO The principal assumption made in the computations is that the cross section of the

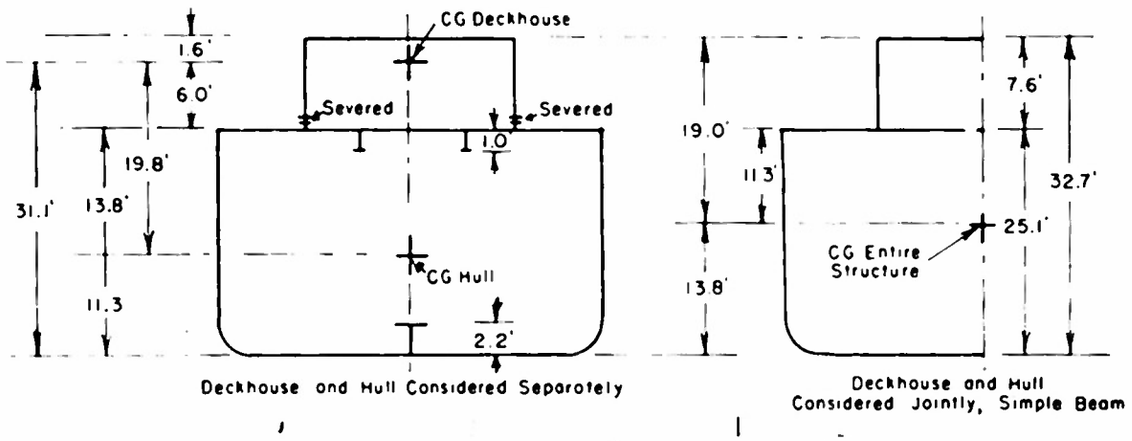

Section Properties* (at Frame 57) Deckhouse $A_1 = 0.75$ ft^2 $I_1 = 5.14$ ft^4

Length = 170 ft Deckhouse extends from Fr. 29 to Fr. 114

Hull Proper $A_2 = 5.49$ ft^2 $I_2 = 499$ ft^4

Deckhouse-Hull Combination $A = 6.24$ ft^4 $I = 762$ ft^4

Vertical Stiffness** of connection between deckhouse and hull = K

$K = 72 \times 10^4$ lb per ft of deckhouse length per ft deflection.

*Computed according to the method of Reference 14 and the PSNY Structural Plan AVP 1013-1111-2.

**This stiffness K was estimated by use of Schade's method for cross-stiffened plating under uniform bending load (Reference 17).

Figure 16 - Parameters Required for Computation of Stress Distribution by the Bleich Method

†The deckhouse is made of steel and has no expansion joints.

A - Navier's stress in hull-deckhouse combination.

B - Navier's stress in Hull (alone).

C - Corrected stress by method of Dr. Hans Bleich.

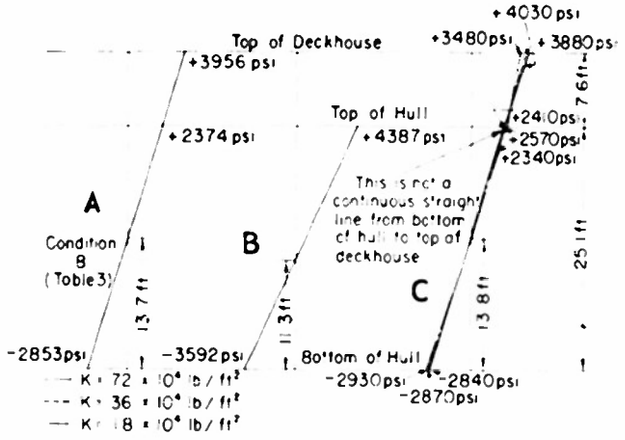

Figure 17a - Stresses for USCGC CASCO in Hogging Condition, Bow Pitching Up

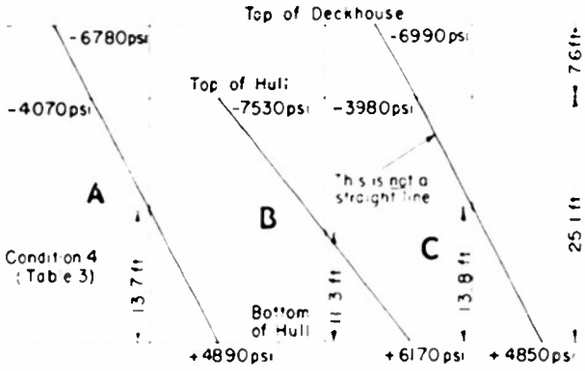

Figure 17b - Stresses for USCGC CASCO in Sagging Condition, Even Keel

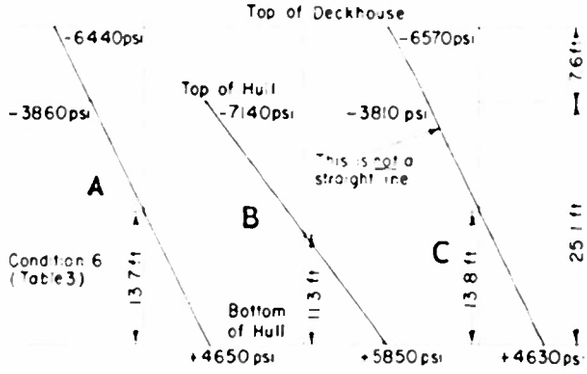

Figure 17c - Stresses for USCGC CASCO in Sagging Condition, Bow Pitching Down

Figure 17 - Stress Distribution in Way of Deckhouse, Frame 71 1/2 (USCGC CASCO)

Computed according to simple beam theory and Bleich's theory.

deckhouse and hull is constant for the length of the deckhouse, Frames 29 to 114, with sectional properties identical with those at Frame 57; see Figure 16. It is believed that this assumption will not affect appreciably the stress distribution near the center portion of the deckhouse.

The stress distribution at the center of the deckhouse, Frame 71 1/2, is plotted in Figure 17 for several of the possible combinations of heaving and pitching motions given in Table 3. For each of these conditions, the stress distribution has been plotted for (a) application of the simple beam theory to the hull-deckhouse combination, (b) application of simple beam theory to the hull alone, and (c) application of Bleich's theory. Inspection of Figure 17 shows that Bleich's analysis gives very nearly the same stress distribution as is obtained with the

assumption of full effectiveness of the deckhouse. Furthermore, the computed location of the neutral axis practically coincides with that based on strain measurements; see Figures 14 and 17. The effectiveness of the deckhouse depends to a large extent on $K^{1/4}$ where K is the vertical stiffness factor defined in Figure 16. The stiffness K cannot be computed with accuracy; however, the hull stresses are not very sensitive to a variation in K; see, for example, Case 8, see Figure 17a, where it is shown that a 4-to-1 variation in K results in a maximum stress variation of only 16 percent.

The ratio of the stress at the main deck to that at the bottom of the keel, near the center of the deckhouse, is 1.22 if the deckhouse is neglected; it is 0.82 utilizing Bleich's theory as well as according to simultaneous strain measurements made at Frame 61 on the CASCO, Figure 14. It may therefore be concluded that the deckhouse does, in fact, contribute materially to the hull girder strength and that Bleich's approach may prove to be practically applicable. It would, however, require more experimental data on different ships with various lengths and structure of deckhouses to reach a definite conclusion as to the validity of this method.

The stresses at Frames 61 and 41 (where the strain measurements were made) have been computed for a number of combinations of the conditions listed in Table 3. The calculated and measured stresses are compared in Table 4. In these computations, the deckhouse is assumed fully effective at Frame 61 and ineffective at Frame 41. The combination on the second line of Table 4 gives the best agreement between measured and computed stresses and, at the same time, provides rather good agreement between the maximum measured variation in pitching angle of 20 deg as against the computed variation (for combination of Conditions 8 and 6) of 16 1/3 deg.

APPENDIX 2

EFFECT OF LOCAL FAILURE ON HULL GIRDER STRENGTH

The strain measurements made near Frame 41 indicated qualitatively that the position of the neutral axis shifted in the upward direction during the whipping motions immediately subsequent to slamming of the bottom of the forward portion of the ship against the sea. This occurrence would be expected if in the vicinity of the strain-gage location, the ship's bottom failed to take a proper share of the bending moment and shear imposed on the hull at that section. It will be shown here that although the over-all hull girder stresses may be quite low, the stresses in the bottom plating may be high, exceeding the yield point of the material under the combined effect of longitudinal compressive loads associated with the bending of the hull together with the lateral pressure load incident to slamming and due to hydrostatic pressure.

The stresses in a typical sheli bottom plate at Frame 41 (strain gage location) were analyzed under the combined effects of a hogging load and normal pressure; see Figure 18. The plate is 24 in. wide by 44.5 in. long and it has a thickness of 0.368 in. It is assumed that the edges of the plate are fixed.

This plate has a buckling strength equivalent to a compressive stress in the plate of about 37,000 psi, in the absence of normal pressures. For the conditions given in Figure 18, which are assumed to approximate the actual conditions on the CASCO, the plate stresses are found to approach the elastic limit for mild steel when the lateral pressure p is 10 psi. It is to be noted that stress concentration has not thus far been considered.

A conservative estimate gives a stress concentration factor of 2 (see Reference 16, p. 136). Plastic deformation can be expected under these conditions, thus resulting in a redistribution of the resisting stresses which would, in effect, make the position of the neutral axis dependent upon the loading, contrary to the assumption of simple beam theory. It is, therefore, apparent that the local strength of the plating may have an appreciable effect on the effective hull girder strength (sectional moment of inertia). Although the entire plating may be effective in resisting the bending moments applied to the hull for some conditions, this may no longer be true under other conditions of loading, even though the applied hull bending moment is the same.

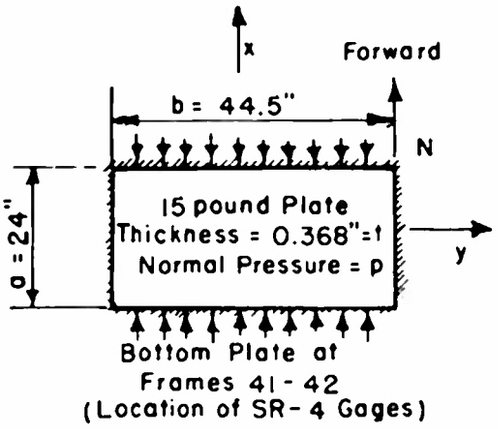

E = Young's Modulus

μ = Poisson's Ratio

t = Plate Thickness

p = Water Pressure

ω_1 = Deflection

σ_A = Direct compressive stress in the plate due to edge compression N lb/in.

1. Buckling Strength of Plate for Zero Pressure ($p = 0$)

From: Timoshenko's "Theory of Plates and Shells," p. 322

Critical Buckling Load $N_c = \dfrac{Et^3}{12b^2(1-\mu^2)} = 13{,}800$ lb/in.

Axial Stress at Buckling $= N_c/t = 37{,}500$ psi $= \sigma_c$

2. Plate Stresses Due to Water Pressure p

Applying Schade's Theory according to Reference 17 and Charts 12 through 14 of Reference 18.

$\sigma_{1B} = 2070\ (p)$ psi $\qquad \sigma_{2B} = 2090\ (p)$ psi

$\sigma'_{1B} = 1460\ (p)$ psi $\qquad \sigma'_{2B} = 1510\ (p)$ psi

$\omega_1 = 0.608 \times 10^{-2}\ (p)$ inches

3. Combined Stresses due to Edge Compression σ_A and Lateral Pressure p

Following the method given by Bleich (Ref. 15, p. 61) a magnification factor "m" is computed. The plate stresses are multiplied by m (m is a function of σ_A) and the resulting stresses are combined with σ_A. This method is an approximation. The results are tabulated below.

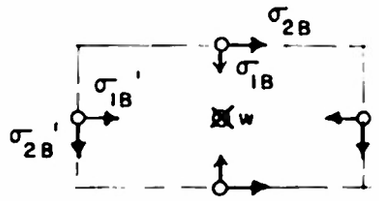

Assume: $\sigma_A = -6000$ psi (due to combined still water and dynamic bending moments acting on ship) then $m = 1.19$

p psi	σ_A psi	$\sigma_x = \sigma_A + m\sigma_{1B}$ psi	$\sigma_y = m\sigma_{2B}$ psi	$\omega = m\omega_1$ inches
0	-6000	- 6,000	0	0
5	-6000	-18,400	-12,400	0.030
10	-6000	-30,600	-24,900	0.061
15	-6000	-43,000	-37,300	0.091

Figure 18 - Plate Stresses Under Combined Lateral Pressure and Edge Compression (For Bottom Plate, Frame 41)

APPENDIX 3

INSTRUMENTATION AND EVALUATION OF INSTRUMENT PERFORMANCE

Each type of instrument will be briefly described in this section together with an evaluation of its performance.

A. THE TMB STRAIN-CYCLE GAGE

This is a device for the statistical determination of the strain history of structures; it will automatically analyze the strain history at the location of the gage in terms of the number of cycles of given strain amplitudes that have occurred. These cyclic variations can be automatically tabulated or classified according to the mean strain about which they took place. Thus, strain data are obtained in a form which can readily be utilized without the necessity of laborious analysis.

The instrumentation comprises two parts, namely, an electrical or mechanical strain gage and an electrical counter. The counter provides an automatic tabulation of the number of cyclic variations of selected strain amplitudes classified according to the mean strain levels about which these cyclic variations occur. To determine the number of variations about a given mean strain level, it is merely necessary to subtract the reading of one counter from that of another.

The principle of operation is probably best illustrated by a simplified diagram (Figure 19a); the main components are (a) a contact bar which is given a linear motion directly proportional to the strain, (b) a series of amplitude contactors which are free to slide as indicated, and (c) a series of zone-level contacts which remain stationary. If the contact bar touches the upper contact point of an amplitude contactor and then touches the lower contact point of the same contactor, a counter will count one unit at the moment the second contact is made. The particular counter which will register is determined by the zone-level contact

Firing Level and Double Amplitude	Equivalent Peak Level and Double Amplitude	Actual Counts	Actual Cycles
1 - 15	4 - 15	3	3
2 - 10	4 - 10	3	3-3 - 0
3 - 5	4 - 5	5	5-3 - 2
1 - 10	3 - 10	0	0
2 - 5	3 - 5	0	0-0 - 0
1 - 5	2 - 5	2	2-0 - 2

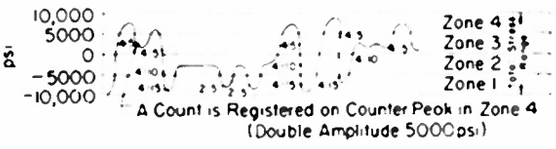

Figure 19a - Sample Analysis of an Arbitrary Strain Variation

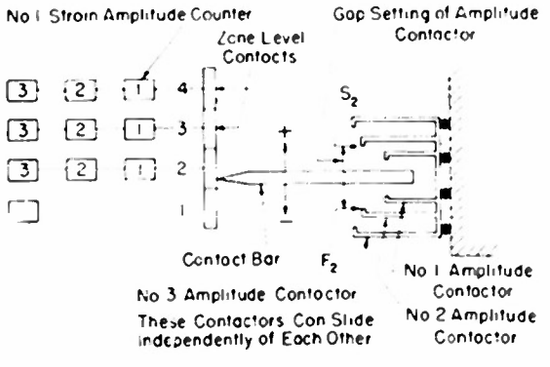

Figure 19b - Diagrammatic Sketch of Strain-Cycle Gage and Counter

Figure 19 - Illustration of Operation and Analysis of Strain-Cycle Gage and Counter

which is touched by the contact bar at the moment of counting. Assume that the unit is in the position shown in Figure 19a for zero strain and that the contact bar moves parallel to itself due to an applied tensile strain. The upper contact points S of the amplitude contactors 1, 2, and 3 are successively touched by the contact bar. The instant contact is made between the contact bar and the point S_2 of the amplitude contactor Number 2, a relay or similar device in an electrical circuit associated with this amplitude contactor is cocked. This relay does not close until the strain, and consequently the contact bar, reverses its direction and contact is made at F_2, at which time the relay closes and a pulse of current is sent through the circuit and channeled via one of the zone-level contacts to the counter corresponding to the Number 2 amplitude contactor. If, for example, the contact bar had been in contact with Section 4 of the zone-level contacts at the instant that the pulse of current was released (contact between F_2 and contact bar), then the Number 2 strain amplitude counter corresponding to the Number 4 zone level would have registered one count. In general, therefore, a count will be registered whenever a strain variation occurs which is equal to or greater than that corresponding to a given gap setting of the amplitude contactors.

The mechanical strain cycle gage used for the CASCO tests is illustrated in Figure 20, and in the photograph, Figure 21. It has a base length of 10 in. and the actual strain is magnified ten times through a lever system. The amplitude contactors are carried by a pivoted and balanced arm which is held in place at any position by a suitable friction pivot. The gage is held to the structure by a predetermined spring force. Rapid temperature changes of the structure were not anticipated. However, temperature effects were to be taken care of by (a) making the gage of the same material as the structure, and (b) minimizing the temperature lag

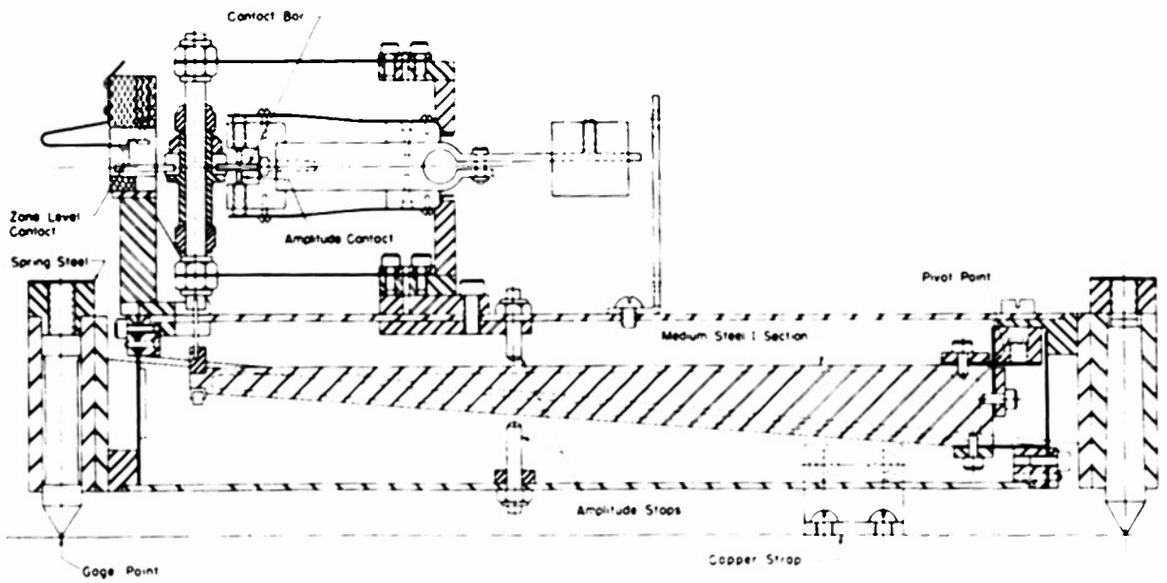

Figure 20 - Section of Strain Cycle Gage

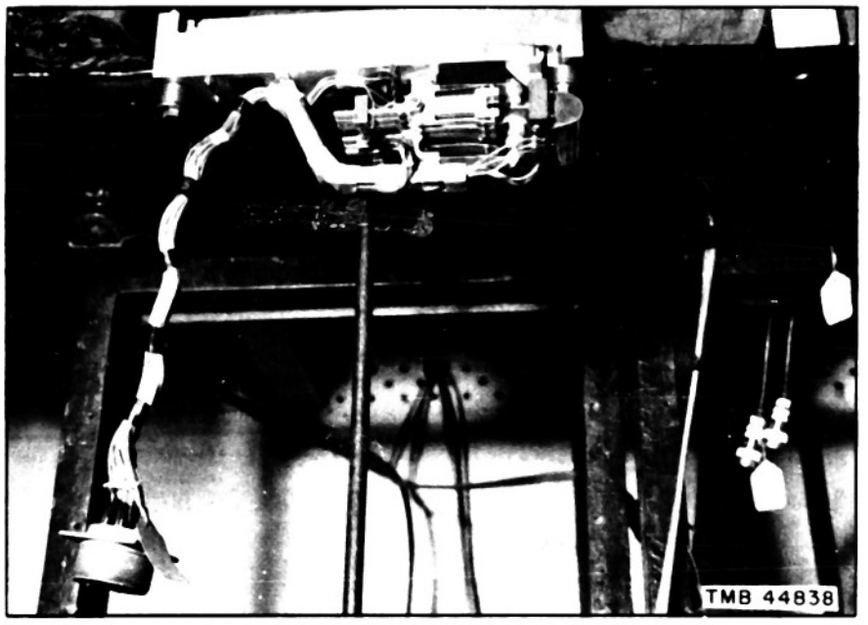

Figure 21 - Mechanical Strain Cycle Gage

between the gage and the structure. The gage is designed to withstand a constant acceleration of 5 g in any direction. The prototype strain cycle analyzer has provision for counting six strain amplitudes and classifying them into six zone levels.

It is seen that the strain cycle gage and counter provide an automatic statistical analysis of the strain variations in a structure over long periods of time at a great savings of time and money over the conventional time-base data. A rough time base can be provided for the strain-cycle data by photographing the counter readings at selected intervals. The units installed on the CASCO comprised three strain-cycle counters which classified the strain variations according to amplitude of the variation only and one counter (strain-cycle analyzer) which classified the strains according to both amplitude of variation and mean level of strain. The latter unit is shown on the right in Figure 7.

The strains experienced by the vessel during the voyage were smaller than expected, therefore most of the counters were not actuated and it was impossible to obtain a good evaluation of the accuracy of these units. It was found, in general, that the mechanical strain-cycle gage operated satisfactorily; however it was accurate enough to classify strains only by amplitude but not by mean level because of its relatively small mechanical amplification.

The electronic counters did have occasional tube failures. The failures were traced to operation of the vacuum tubes at excessive temperatures. The circuits have been redesigned and the counters rebuilt to operate at reduced currents and temperatures and do perform satisfactorily.

For general application, the mechanical strain gage should be replaced by an SR-4 or similar electrical strain gage working into a mechanical follow-up system which will, in time, actuate the counters. Development of such a device is nearly completed.

The basic idea of the strain cycle gage can be utilized in other applications where it is desired to count cyclic variations, for example, in the cyclic analysis of voltages, currents, pressures, strains, temperatures and atmospheric conditions.

B. TIME TOTALIZER

If it is found that fatigue is not a significant consideration in a particular problem, then it would be unnecessary to classify the strain data as before (by amplitude and/or mean level). It may be sufficient to know what percentage of the total operating time the strain falls within given limits. To provide this information another instrument has been designed and built which performs a measuring, analyzing, and totalizing function. This instrument is called a time totalizer or, in this particular case, a strain totalizer; see Figure 22. The essential components are a strain gage, a switching or classifying device, and a series of clocks. The operation is as follows: The output of a strain gage is used to change the bias of a vacuum tube. Each vacuum tube will conduct current when its grid voltage exceeds a fixed value, which value is, in turn, set to correspond to a definite strain. Each tube controls a clock which will run as long as the tube is conducting current. Therefore, the total time indicated by any clock indicates the total time that the strain has exceeded the value corresponding to that particular clock. The total time that the strain was in a given region is given by the difference of the clock readings for the two strains defining that region. These data can be represented immediately and conveniently by a simple graph.

The accuracy of this device depends to a great extent on the rapidity of strain variations and on the time delay of the clocks. In the present installation the same strain gage that was part of the strain cycle counter in the strain totalizer is utilized. However, almost any electrical or mechanical gage could be adapted to the strain totalizer.

The totalizer installation can be seen in Figure 7. The magnitude of the strains experienced was insufficient to evaluate this device.

C. TMB AUTOMATIC SHIP'S MOTION RECORDER

A detailed description of this device is given in TMB Report 777.[8] Shown in Figure 23, it is essentially an amplifier and recorder which has provision for automatic sampling and which is designed to operate continuously for weeks on shipboard without necessitating attention. It is called the *TMB Automatic Ship's Motion Recorder* but could be used for purposes other than that indicated by its name. It should be remembered that this is the first and only model built and that additional features will be added to later models. The recorder operates on a 110-volt alternating current and is designed to record the ship's rolling and pitching acceleration, its linear acceleration, and the rolling and pitching angles. Since it is desired to record only the rather low-frequency variations associated with the oscillatory motion of

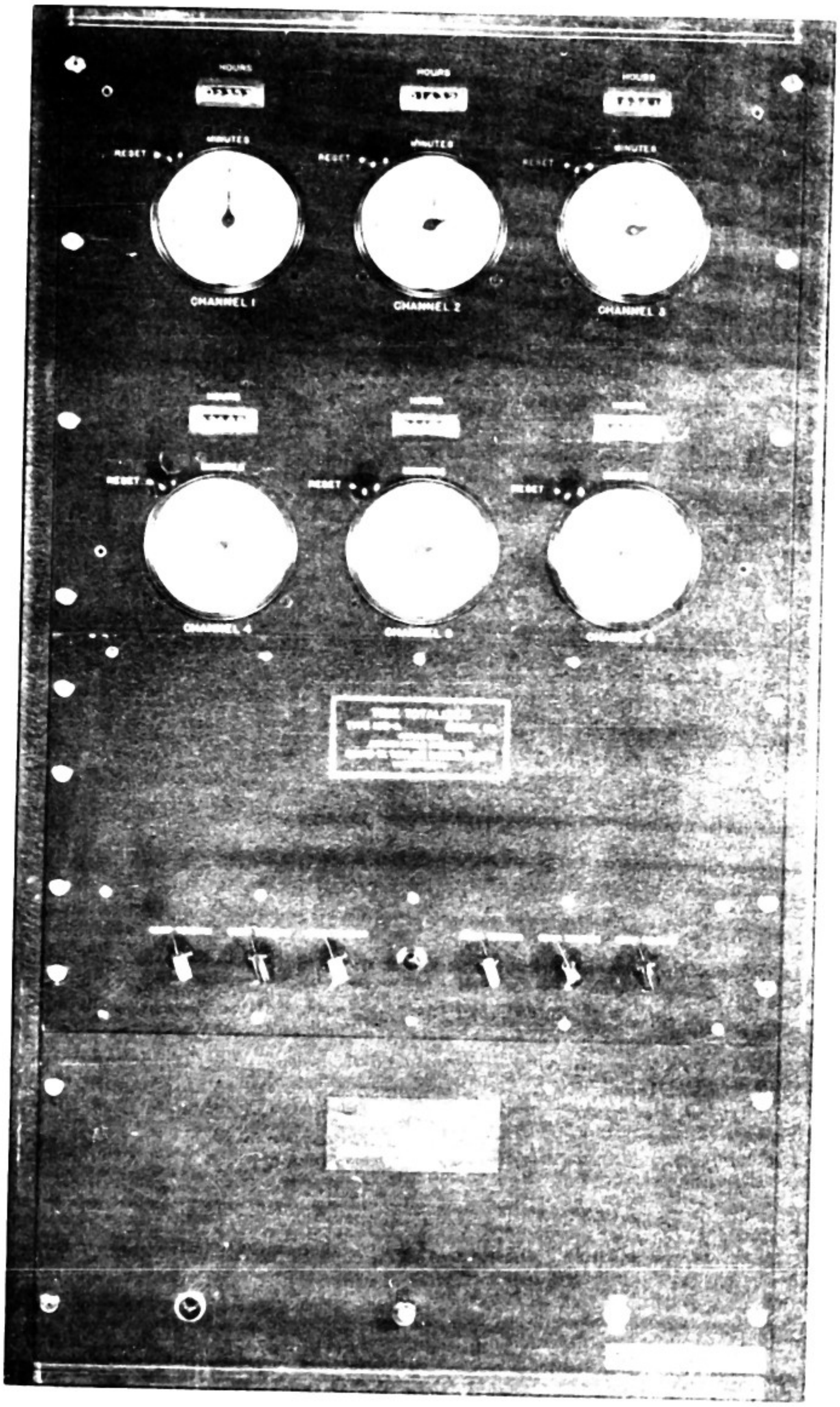

Figure 22 - Time Totalizer

the vessel, that is, rolling, pitching, and heaving [illegible], [illegible]
must be attenuated.

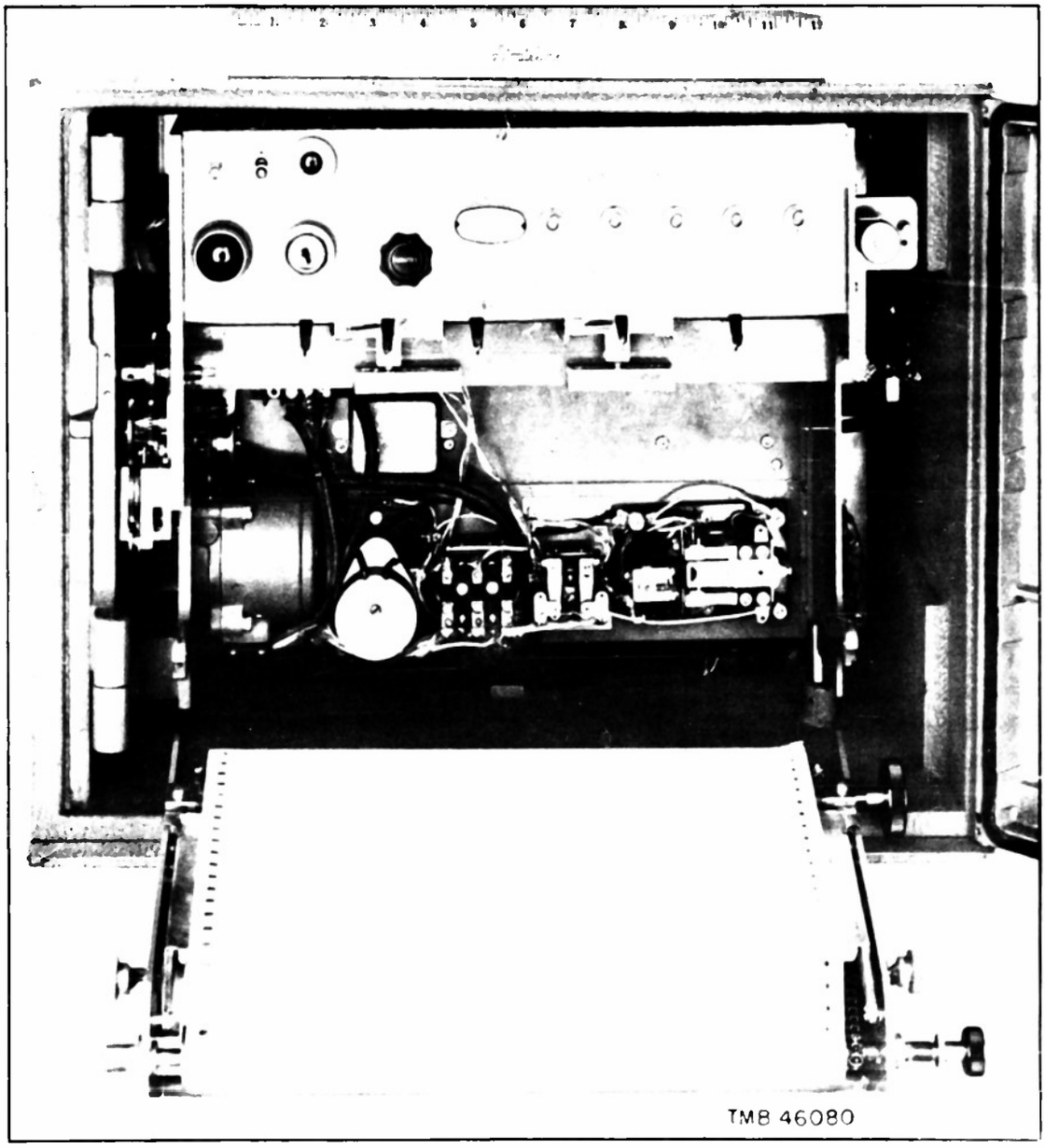

Figure 23 - TMB Automatic Ship's Motion Recorder

The voltage output of each transducer is amplified and its phase is shifted to provide maximum power input into one phase of a two-phase motor; the other phase is connected directly across the line. The direction and amount of rotation of the motor are directly proportional to the direction and magnitude of the transducer signal. The motor operates a null-balance system, hence there is no appreciable error due to lack of voltage regulation in the power supply. The two-phase motor actuates a standard type of pen drive. The pens scribe on a plastic-coated recording paper.

The paper drive is actuated by a set of cams as follows:

1. The paper drive operates automatically; the pens are actuated for a preselected period at regulated intervals, say for 2 min. out of every hour.

2. The recorder will record for any desired continuous period up to 2 hr by manually turning a timer knob. At the end of the period the automatic cycling will take over.

3. The recorder will run continuously if desired.

The chart speed used is either 1 or 1/2 in/min; 100 feet of paper is sufficient to permit up to 50 days' operation without reloading the magazine. In use it is intended to select the optimum sampling interval and sampling duration for the particular problem under consideration.

Additional features can readily be added to the present unit. For example, the recording may be controlled by the magnitude of the quantity to be measured or by some other quantity. A definite limitation of the recorder is its upper limitation of frequency response.

The transducers used with the recorder were Schaevitz accelerometers for the acceleration measurements and the stable element and synchro follow-up system of the New York Materials Laboratory Ship's Motion Recorder for the roll and pitch channels. The transducers and the recorder gave satisfactory service during the tests.

D. SHIP'S MOTION RECORDER BUILT BY THE NEW YORK MATERIALS LABORATORY

This recorder is a self-contained unit comprising a recorder, a stable element, and four synchro channels. It is intended to record angles of roll and pitch, ship's heading, and ship's speed. The stable element furnishes the input for the roll and pitch channels; the ship's gyro compass and log provide the input for the course and speed channels. In the shipboard installation aboard the CASCO, the Taylor Model Basin and the New York recorders were wired in parallel and actuated by the control system of the TMB unit; in this manner the two units gave simultaneous data. The stable element of the New York unit was utilized for the angle of roll and pitch inputs of the TMB recorder.

The pens of the New York Materials Laboratory recorder require refilling with ink about every day and occasionally become clogged. The pen indicating the course of the ship jammed whenever it reached an extreme position in its travel. There was some backlash in the gearing between the synchros and the pens.

E. DIAPHRAGM PRESSURE GAGE

This gage, shown in Figures 24 and 25, is installed with its face flush with the outside of the ship's plating to measure the water pressure at that point. The gage consists of a gage cup, a differential transformer with positioning adjustment, and a protective cover; see Figure 24. The diaphragm is 1 in. in diameter, 0.024 in. thick, and carries a small soft iron core

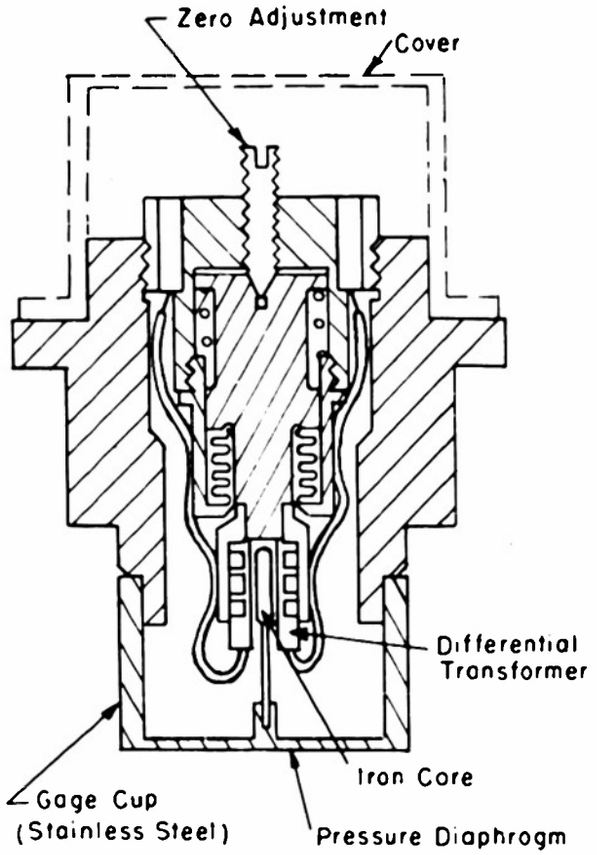

Figure 24a - Drawing of Pressure Gage

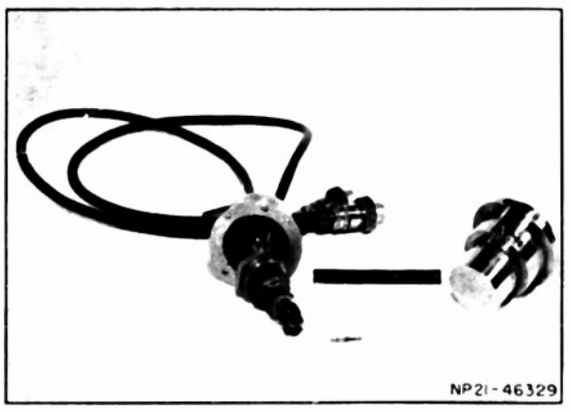

Figure 24b - Photograph of Disassembled Pressure Gage

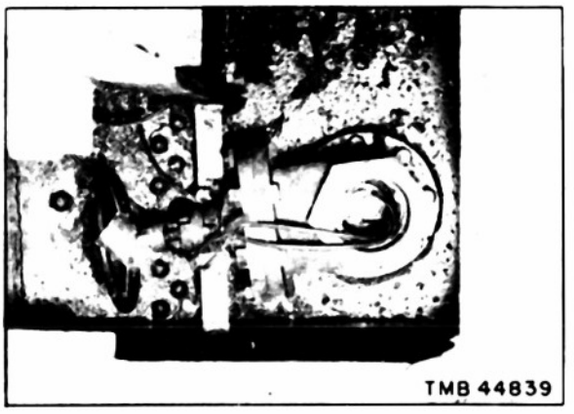

Figure 24c - Photograph of Pressure Gage Installation on USCGC CASCO

Figure 24 - Diaphragm Pressure Gage Which Utilizes a Differential Transformer as the Sensitive Element

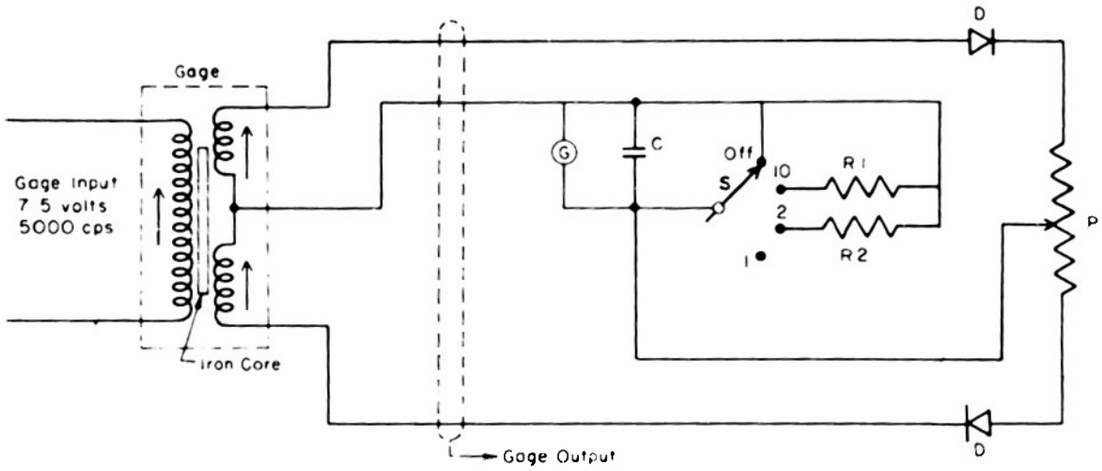

C	Condenser, 40μf (TMB Stock No. 16-0540)
D	Diode, IN34
G	Galvanometer, 30μA
P	Potentiometer, 10 ohms
R_1	Resistor, 4.4 ohms
R_2	Resistor, 40 ohms
S	Selector Switch

1. Over-all Sensitivity of Pressure Gage - Circuit Combination:
   Attenuator (1) 75 mils deflection of galvanometer/psi pressure
   (2) 40.5 mils deflection of galvanometer/psi pressure
   (10) 8.8 mils deflection of galvanometer/psi pressure
2. Natural Frequency of Pressure Gage: Approx. 1200 cps
3. Over-all Sensitivity of 10-in. Electromechanical Strain Gage - Circuit Combination:
   Attenuator (1) 240 mils deflection of galvanometer/1000 psi stress
   (2) 125 mils deflection of galvanometer/1000 psi stress
   (3) 25 mils deflection of galvanometer/1000 psi stress
4. Immersion of Cables in Salt Water has no effect on Sensitivity.

Figure 25 - Circuit Diagram and Characteristics of Diaphragm Pressure Gage and 10-in, Electromechanical Strain Gage

attached to its center. Pressure acting on the diaphragm will cause it to deflect, thus deflecting the iron core relative to the gage housing which, in turn, changes the flux linkage between the primaries and secondaries of a small transformer and induces a voltage change proportional to the deflection of the diaphragm. The primary of the differential transformer is excited with a 5000-cps voltage from a Hewlett-Packard oscillator; the output of the secondaries is then rectified and impressed on a string galvanometer; see Figure 25. The circuit is quite simple and sensitive, but the frequency response falls off at 60 cps due to the effect of the galvanometer response. The natural frequency of the gage is about 1200 cps. The gage was designed

to be linear up to a pressure of 20 psi and to be reasonably linear, within 10 percent, up to 100 psi. The gage body, which is made of stainless steel, showed no evidence of deterioration after about a 50-day exposure to sea water. The diaphragm, however, acquired a permanent set of about 0.018 in. due to large impact pressures. Calculations using the theory of plasticity indicate that the equivalent static pressure causing such a set was in excess of 265 psi.

The gage and gage circuit performed satisfactorily throughout the entire tests. If, however, the gage is to be located in a region of high impact pressures, the diaphragm must be designed to withstand equivalent static pressures of the order of several hundred psi without acquiring a permanent set.

F. TEN-INCH STRAIN GAGE

This gage (Figure 6) is simply a strain gage of 10-in. base length having no mechanical amplification. The relative motion between the knife-edge points moves the core of a differential transformer, thus changing the flux linkage between the primary and secondary windings in proportion to the strain. The electrical circuit is identical with that for the diaphragm pressure gage. Electrically, the performance of the gage was satisfactory, but, unfortunately, no usable data were obtained because, through an oversight, the knife edges had not been hardened and consequently the gage points slipped relative to the structure when straining occurred.

G. SR-4 STRAIN GAGE

The SR-4 wire-resistance strain gage (Figures 5, 6, and 26) is well known and need not be discussed here. The gages were oriented to measure the longitudinal strain in the keel and in the main-deck longitudinals. They were waterproofed and then covered with a steel plate for protection. The gages were electrically connected in a bridge circuit, see Figure 26, and the output was recorded on a Consolidated oscillograph simultaneously with the output of the pressure gage. All gages performed satisfactorily throughout the test period. It should be noted, however, that they were not immersed in water at any time during the tests.

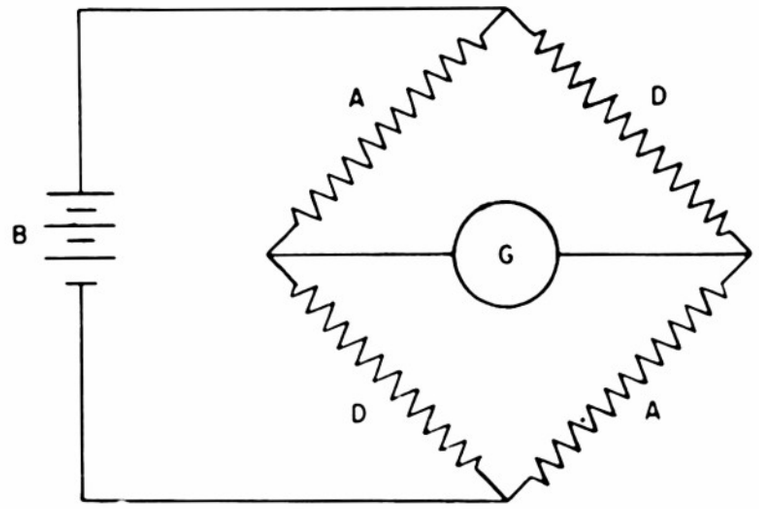

Over-all-sensitivity: 18.75 psi per mil deflection of 13μA galvanometer trace

Galvanometer Data:

Mfg..	Consolidated
Model:	7-115
Sensitivity:	13μA/inch
Frequency Response:	Flat $\pm$ 5 percent from 0 - 60 cps

SR-4 Gage Data:

Type:	A-14
Resistance:	500 $\pm$ 3 ohms

Figure 26 - Circuit Diagram for SR-4 Strain Gage Installation

APPENDIX 4

STATISTICAL PRESENTATION OF DATA FROM TESTS ON USCGC CASCO

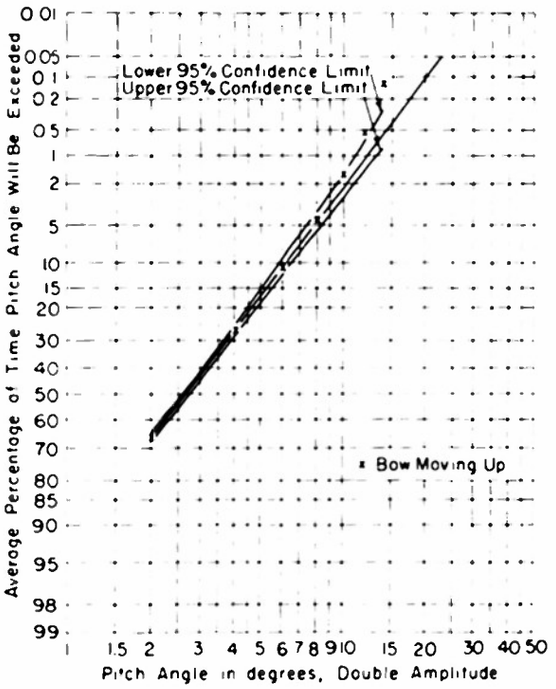

Figure 27a - Pitch Angle

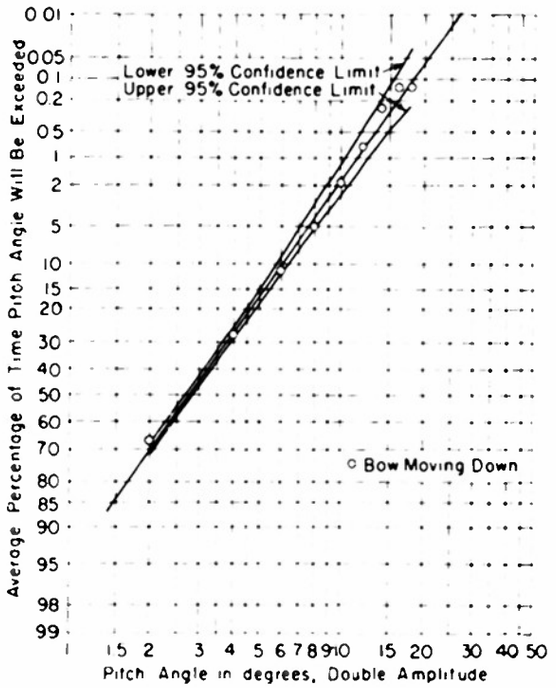

Figure 27b - Pitch Angle

Figure 27 - Statistical Presentation of Ship-Motion Data

The "confidence limits" also known as "probability levels" denote the limits between which 95 per cent of the experimental measurements would fall if a great number of tests were made (tests assumed to be made under the same condition).

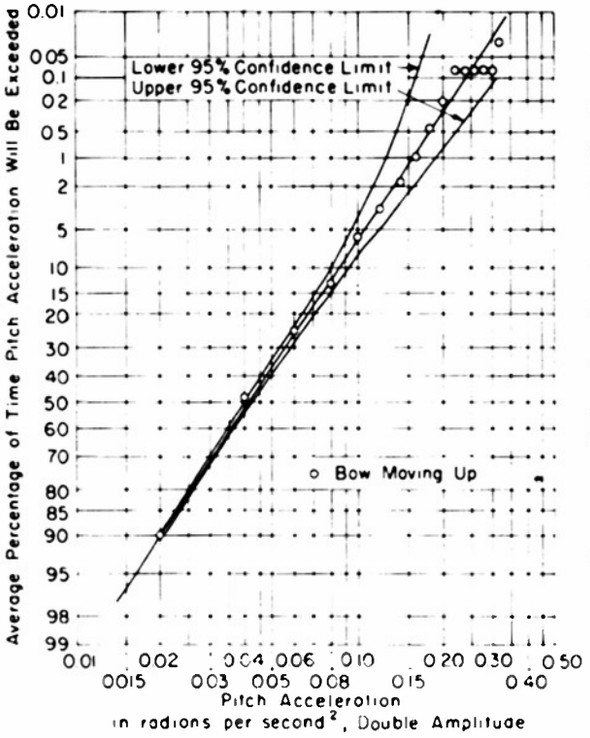

Figure 27c - Pitch Acceleration

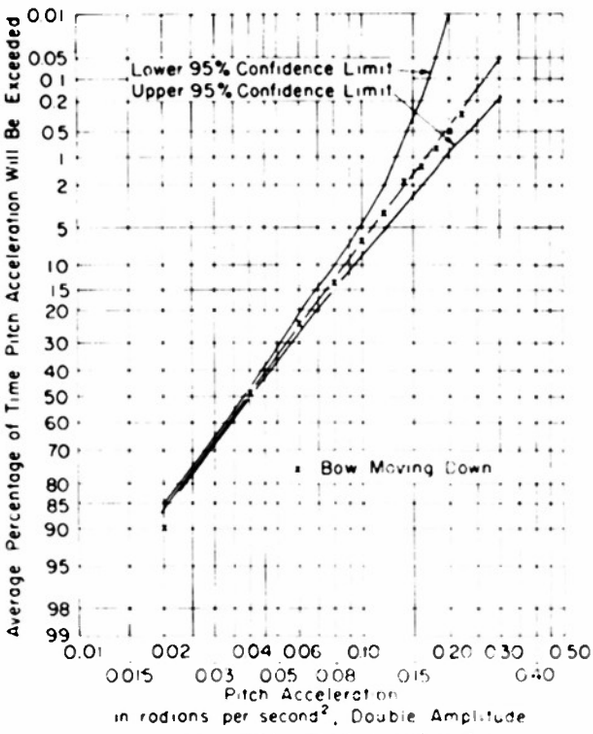

Figure 27d - Pitch Acceleration

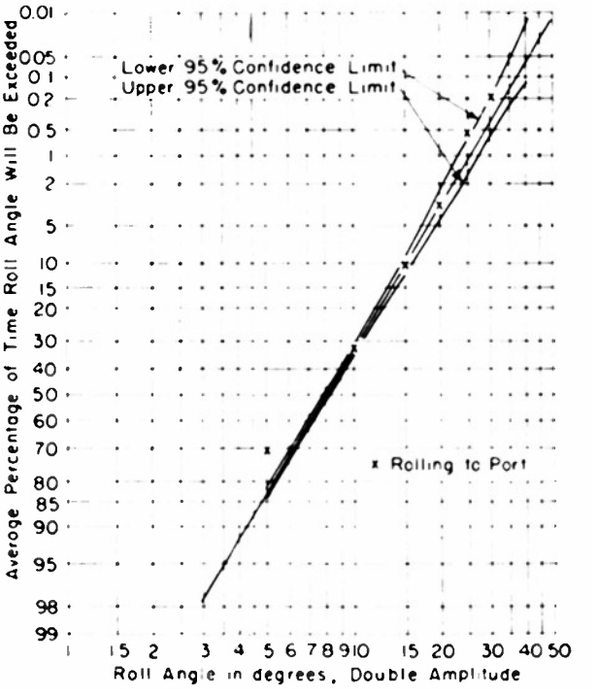

Figure 27e - Roll Angle

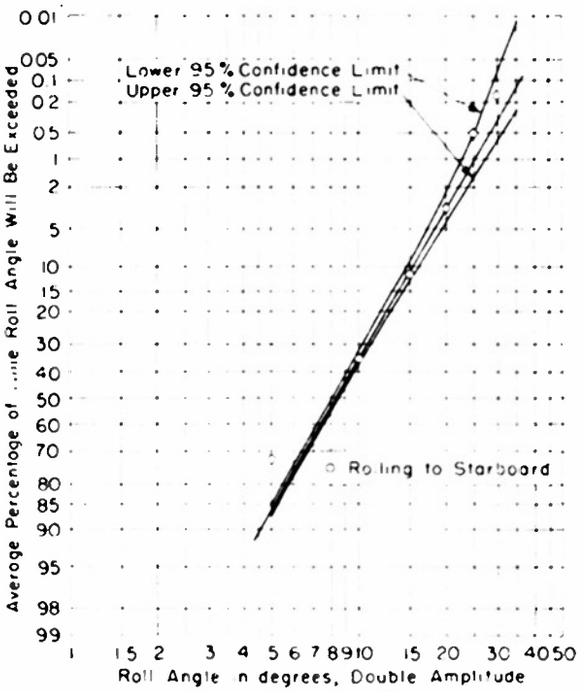

Figure 27f - Roll Angle

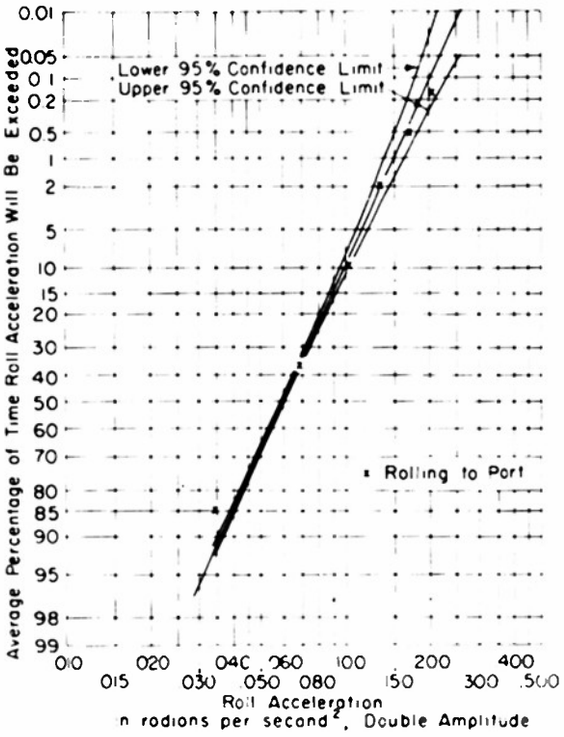

Figure 27g - Heave Acceleration

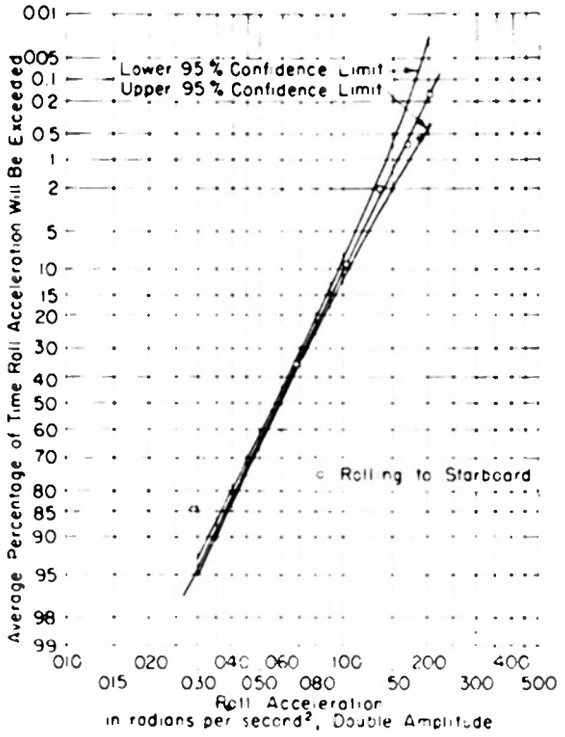

Figure 27h - Heave Acceleration

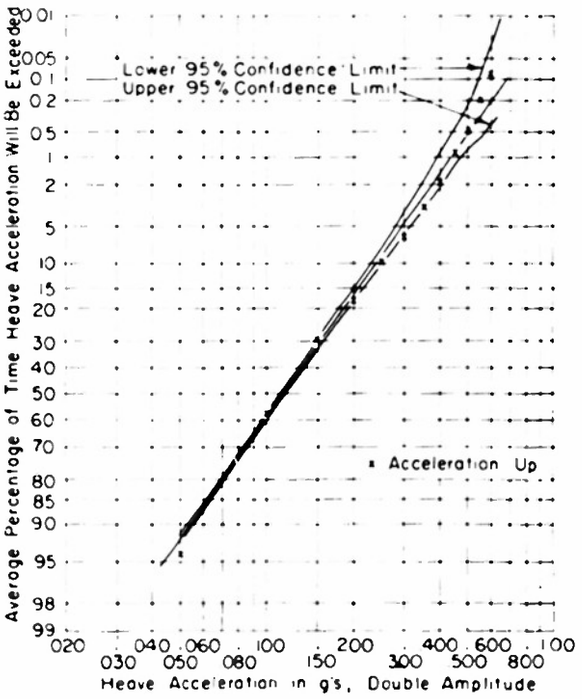

Figure 27i - Roll Acceleration

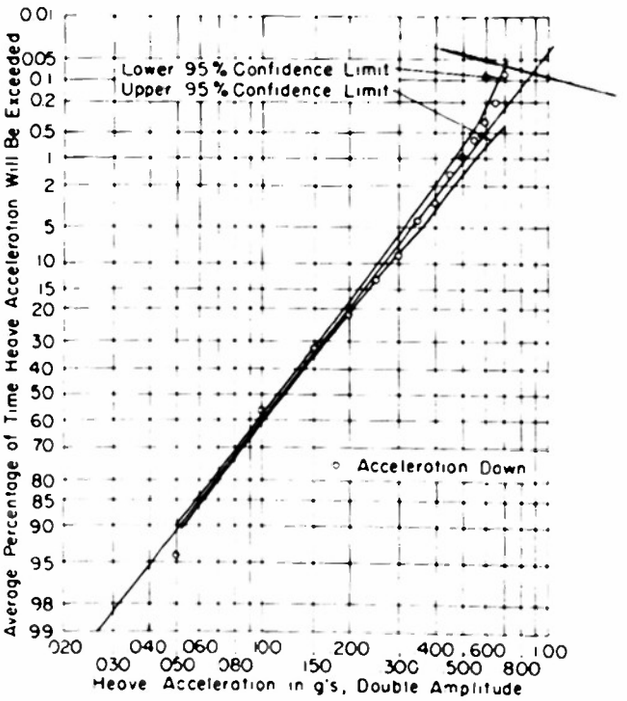

Figure 27j - Roll Acceleration

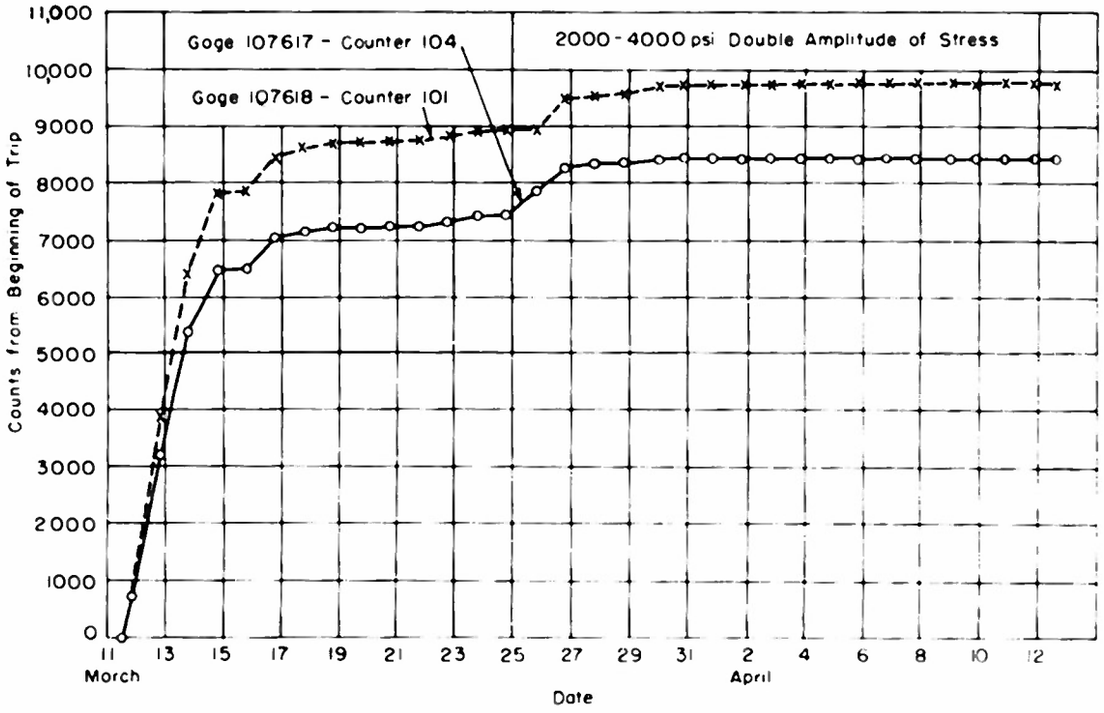

Figure 28a - Cumulative Total of Strain Cycles with Double Amplitudes of 2000 to 4000 PSI

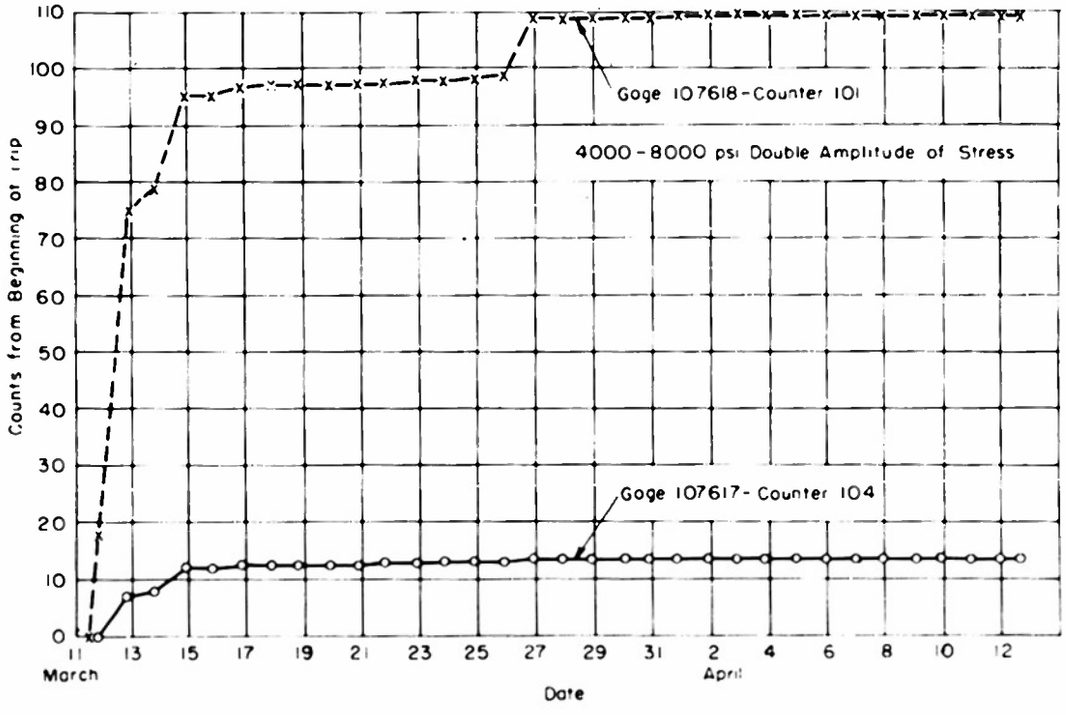

Figure 28b - Cumulative Total of Strain Cycles with Double Amplitudes of 4000 to 8000 PSI

Figure 28 - Cumulative Counts of Longitudinal Stresses in Keel (Station 3)

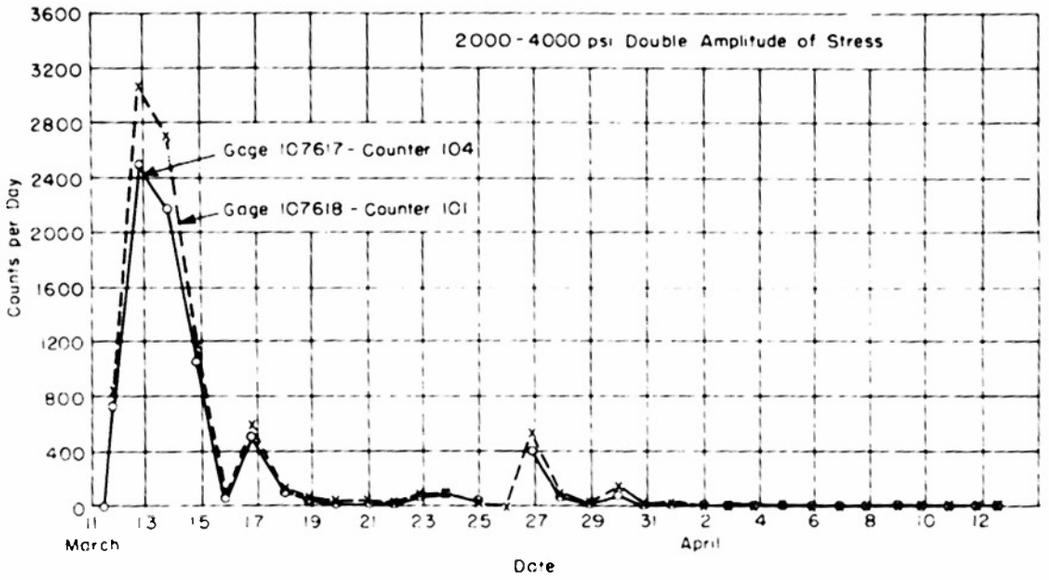

Figure 29a - Occurrence Rate of Strain Cycles with Double Amplitudes of 2000 to 4000 PSI

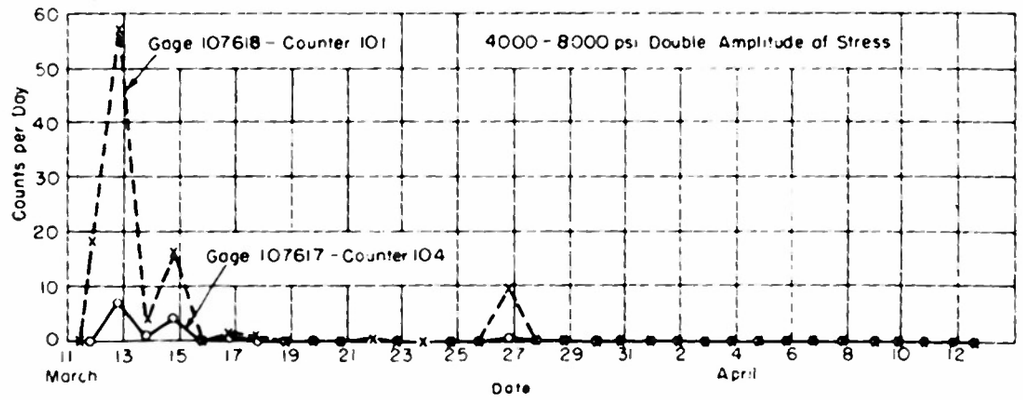

Figure 29b - Occurrence Rate of Strain Cycles with Double Amplitudes of 4000 to 8000 PSI

Figure 29 - Incremental Counts of Longitudinal Stresses in Keel (Station 3)

ACKNOWLEDGMENTS

Much credit is due Mr. Q. R. Robinson of the Taylor Model Basin Vibrations Division for the careful work and enthusiasm which he devoted to the experimental phases of this project, especially during the sea trials. Much of the record analysis was performed by Messrs. Q. R. Robinson, D. Messer, J. Higgins and R. Milam all of the Vibrations Division.

The statistical probability patterns were computed by Messers. A. S. Marthens and I. B. Altman of the Bureau of Ships (Code 373).

REFERENCES

1. BuShips ltr S29-7(442-440-330) to TMB dtd 21 June 1948.

2. Jasper, N.H., "A Statistical Approach to the Longitudinal Strength Design of Ships," Jour. ASNE, Vol. 62, No. 3, August 1950.

3. Jasper, N.H., "A Statistical Approach to the Measurement and Analysis of Experimental Data on Structures," Jour. ASNE, Vol. 63, No. 3, August 1951.

4. BuShips ltr S29-7(442) over Ser 442-131 to Commandant, U.S. Coast Guard dtd 16 November 1950.

5. Commandant, U.S. Coast Guard ltr ENE to Chief, BuShips dtd 28 November 1950.

6. Allnutt, R.B., and Mintz, F., "Instruments at the David Taylor Model Basin for Measuring Vibrations and Shock on Ship Structures and Machinery," TMB Report 563, July 1948.

7. "Instructions for Recording and Coding Main Meteorological Observations in the New International Code," Weather Bureau, U.S. Department of Commerce, 1948.

8. Jasper, N.H., "The TMB Automatic Ship's Motion Recorder," TMB Report 777, October 1951.

9. Comstock, J.P., "Introduction to Naval Architecture," Simmons-Boardman Publishing Co., New York, 1944.

10. Watts, I., Rankine, W.J.M., Barnes, F.K., and Napier, J.R., "Shipbuilding, Theoretical and Practical," McKenzie, London, 1866.

11. Gleyzal, A., "Plastic Deformation of a Circular Diaphragm under Pressure," Jour. Appl. Mech., Vol. 15, No. 3, September 1948.

12. Rossell, H.E. and Chapman, L.B., "Principles of Naval Architecture," SNAME, New York, 1947.

13. Jasper, N.H., "Dynamic Loading of a Motor Torpedo Boat (YP 110) During High-Speed Operation in Rough Water," TMB CONFIDENTIAL Report C-175, September 1949.

14. BuShips Plan No. AVP 1011-2907-1, "Weight and Buoyancy Curves."

15. Bleich, H., "A Study of the Structural Action of Superstructures on Ships," BuShips Contract NObs-50538, Report for the Ship Structure Committee, 21 December 1951.

16. "The Design and Methods of Construction of Welded Steel Merchant Vessels," Report of U.S. Board of Investigation to Inquire into the Design and Methods of Construction of Welded Steel Merchant Vessels, U.S. Government Printing Office, 15 July 1946.

17. Schade, H.A., "Design Curves for Cross Stiffened Plating under Uniform Bending Load," Proc. SNAME, 1941.

18. Bleich, F. and Ramsey, L.B., "A Design Manual on the Buckling Strength of Metal Structures," SNAME Tech. Res. Bulletin 2-2, September 1951.

INITIAL DISTRIBUTION

Copies	
17	Chief, Bureau of Ships, Technical Library (Code 327), for distribution: 5 Technical Library 1 Naval Architecture Planning Coordinator (Code 318) 1 Applied Science Division (Code 370) 1 Statistical Quality Control Branch (Code 373), Mr. Marthens 1 Ship Design Division (Code 410) 1 Preliminary Design and Ship Protection (Code 420) 1 Hull Design (Code 440) 2 Scientific - Structural and Hydromechanics (Code 442) 1 Ship Technical Division (Code 500) 1 Electrical Branch (Code 560) 1 Electronics Design and Development Division (Code 810) 1 Radar Branch (Code 820)
1	Bureau of Aeronautics
1	Director, U.S. Naval Research Laboratory, Anacostia, Washington 25, D.C.
1	Commander, U.S. Naval Ordnance Laboratory, Mechanics Division, White Oak, Silver Spring 19, Md.
1	Commander, New York Naval Shipyard, Material Laboratory, Brooklyn 1, N.Y., Attn: Mr. G. Dashefsky
1	Commander, Puget Sound Naval Shipyard, Code 251, Bremerton, Wash.
1	Commander, Mare Island Naval Shipyard, Vallejo, Calif.
1	Commander, Boston Naval Shipyard, Boston 29, Mass.
1	Commander, Portsmouth Naval Shipyard, Portsmouth, N.H.
1	Commander, Norfolk Naval Shipyard, Portsmouth, Va.
1	Director, U.S. Engineering Experiment Station, Annapolis, Md.
1	United States Weather Bureau, 24th and M Sts., N.W., Washington 25, D.C.
3	Commandant, U.S. Coast Guard, Headquarters, Washington 25, D.C.
1	Commanding Officer, U.S. Naval Medical Research Institute, National Naval Medical Center, Bethesda 14, Md., Attn: Dr. D.E. Goldman
1	Newport News Shipbuilding and Drydock Co., Newport News, Va., Attn: Mr. Comstock
1	Director, Experimental Naval Tank, Department of Naval Architecture and Marine Engineering, University of Michigan, Ann Arbor, Mich.
1	Director, Applied Physics Laboratory, Johns Hopkins University, 8621 Georgia Ave., Silver Spring, Md.
10	Secretary, American Society of Naval Architects and Marine Engineers, 29 W. 39th St., New York, N.Y.

Copies

1	Engineering Societies Library, 29 West 39th St., New York, N.Y.
1	Professor John E. Younger, School of Engineering, University of Maryland, College Park, Md.
1	Dr. K.S. M. Davidson, Director, Experimental Towing Tank, Stevens Institute of Technology, Hoboken, N.J.
1	Dr. Hans Bleich, School of Engineering, Columbia University, New York, N.Y.
9	British Joint Services Mission (Navy Staff), P.O. Box 165, Benjamin Franklin Station, Washington, D.C.
1	U.S. Naval Attache's Office, London, England, Attn: CDR L.A. Rupp
1	Director, British Shipbuilding Research Association, 5 Chesterfield Gardens, Curzon Street, London, W. 1, England
1	Dr. G.P. Weinblum, Ingenieur Schule, Berliner Tor 21, Z 620, Hamburg, Germany
1	Prof. Dr. Ing. G. Schnadel, 58 Ferdinandstr, Hamburg 1, Germany